The effects of selective attention on sensory encoding and choice activity across auditory cortex

By

JENNIFER MOHN
DISSERTATION

Submitted in partial satisfaction of the requirements for the degree of

DOCTOR OF PHILOSOPHY

in

Neuroscience

in the

OFFICE OF GRADUATE STUDIES

of the

UNIVERSITY OF CALIFORNIA DAVIS

Approved:

Gregg Recanzone, PhD, Chair

Mitchell Sutter, PhD

Jochen Ditterich, PhD

Timothy Hanks, PhD

Christoph Schreiner, PhD

Committee in Charge

2021

Table of Contents **Page**

List of Tables and Figures **Page**

Abstract

The effects of selective attention on neural encoding and choice-related activity across auditory cortex

Jennifer L. Mohn

Selective attention helps us to make sense of noisy sensory environments by prioritizing representation of stimuli relevant to behavioral demands while ignoring a wide array of distractors. Yet, the neural mechanisms that underlie attention remain poorly understood. In the following studies, we aim to assess how selective attention effects encoding of amplitude modulated noise (AM) in single neurons from primary (A1) and secondary (middle lateral belt, ML) auditory cortex of Rhesus macaques. We assess two different forms of attention – feature-selective attention and intermodal attention – and compare to previous task-engagement studies to probe distinctions between arousal and selective attention effects on neural activity. Further, we assess choice-related activity during these behavioral tasks and how such activity is modulated by attentional contexts. We found that feature-selective attention did not significantly affect the encoding of AM in either A1 or ML neurons. However, choice-related activity did shift between attentional conditions in both A1 and ML, suggesting that choice-related activity cannot be reflective of motor preparation alone. During a novel intermodal attentional task, we found that AM discrimination was significantly improved when animals were presented with unimodal auditory stimuli, compared to bimodal audiovisual stimuli. However, there were few differences in AM discrimination between bimodal conditions when subjects were attending to the auditory component of the stimulus rather than ignoring it to attend the visual component. These findings suggest that the effects seen are largely an effect of distracting stimuli, rather than selectively attending to auditory stimuli over visual stimuli. Finally, we found that choice-related activity was stronger on trials when audiovisual stimuli provided congruent evidence towards a response rather than when information from the two modalities was in conflict, suggesting that choice-related activity is modulated by reward-expectation.

Acknowledgements

I would like to thank the Sutter lab, past and present: Mitch, for fostering my scientific independence; Kevin, you were such an integral part of my training; I truly can't imagine having done this without you; Jeff, for being a programmer extraordinaire and always being quick to answer my cries of emergency when things were breaking; Josh, for showing me the ropes at the very beginning; Tyler, for keeping things running these past few years; and all our wonderful undergraduates. To my committee, thank you for your support all these years. I have no doubt that the contents of this dissertation and my science in general is better because of you all. To our amazing veterinary staff, Dr. Rhonda and Dr. Kacie most notably, the care you provide our animals and the assurance you bring to stressful situations is so appreciated. Many thanks to Ken Britten, Jochen Ditterich, and Henry Alito for providing insight into dot motion training and fixation training for this auditory person who decided to foray into the visual realm. To my amazing cohort who were amazing scientific support and even better friends; I am so thankful to have such a lovely and fun group of people. To my swim family at Davis Aquatic Masters, the support and reminder of normal life were absolutely critical to me during my time in Davis. So much love and thanks to my family who supported me on this journey and helped me grow into the person I am today. To my pets, Kinje, Oli and Rosy, who provided much needed cuddles and laughs every day. And finally, to my partner, Tim, for your love and support – particularly during this last year that could have been miserable, but instead was one of the best years yet – I cannot thank you enough. You make me a better person and scientist every day, I love you.

General Introduction

The neural mechanisms underlying attention have long been of interest to neuroscientists (Hocherman et al. 1976; Hubel et al. 1959). Attention has been shown to change neural firing rates (Benson and Hienz 1978; Hocherman et al. 1976; Miller et al. 1972), alter tuning curve properties (Fritz et al. 2003, 2007; Fritz 2005), increase neural discriminability of stimuli (Niwa et al. 2012a, 2015), and alter correlated variability within neural populations (Cohen and Maunsell 2009; Downer et al. 2015, 2017). In auditory cortex, studies of attention have largely employed an active/passive task paradigm, in which subjects are presented with sounds and they alter between passively listening to the sounds and performing some sort of task related to the sounds (Angeloni and Geffen 2018; Atiani et al. 2014; Buran et al. 2014; Carcea et al. 2017; Fritz et al. 2003, 2007; Lee and Middlebrooks 2011; Niwa et al. 2012a; Osmanski and Wang 2015). While these studies have certainly improved our understanding of behavioral changes auditory cortical responses, this behavioral paradigm makes it difficult to disentangle arousal effects from more specific forms of attention, such as selectively attending to one sound source while ignoring others.

Investigations into selective attention are less common in auditory cortex (Downer et al. 2017; O’Connell et al. 2014; Schwartz and David 2018). In the visual system, it has been shown that selective attention can change response magnitude, latency variability, as well interneuronal correlated variability (Cohen and Maunsell 2011; Desimone and Duncan 1995; Maunsell 2015; Mirabella et al. 2007; Rodgers and DeWeese 2014; Wimmer et al. 2015). However, it remains unclear if similar mechanisms are employed in the auditory system. The studies in this dissertation seek to discern if and how two forms of selective attention – feature-selective attention and intermodal attention– modulate the encoding of sounds in the auditory cortex. Further, we ask the extent to which these attentional mechanisms may differ between hierarchical stages of processing by comparing neural responses from a primary auditory cortical area (A1) and a secondary area (middle lateral belt, ML) from Rhesus macaques performing auditory attention tasks.

Both studies presented here utilize sinusoidally amplitude modulated broadband noise (AM) to assess how sensory encoding is modulated by attention. Sound envelope amplitude modulation is a saliant feature of natural sounds including speech and animal vocalizations (Elliott and Theunissen 2009; Gervain and Geffen 2019; Singh and Theunissen 2003), in addition to being an important feature in sound segregation (Bregman 1994; Grimault et al. 2002). AM stimuli can be encoded with both a rate code and phase-locking temporal code. Generally, phase-locking encoding tends to be better in earlier stages of processing whereas AM encoding seems to shift to a primarily rate code at higher processing stages (Bieser and Mueller-Preuss 1996; Gao and Wehr 2015; Johnson et al. 2012, 2020; Joris et al. 2004; Schreiner and Urbas 1988; Yin et al. 2011). Further, encoding of AM has been relatively well studied in auditory cortex (Hoglen et al. 2018; Johnson et al. 2012, 2012, 2020; Malone et al. 2015; Overton and Recanzone 2016; Schreiner and Urbas 1988; Yin et al. 2011), making it a good stimulus to assess how the encoding of AM changes with behavioral context.

In the first study of this dissertation, we assessed how amplitude modulation detection changed when subjects were cued to attend to changes in that feature, compared to when they were cued to attend to changes in the spectral content of the stimulus. Notably, both AM and spectral features can be encoded using a rate code within the same neuron in auditory cortex. Therefore, a rate code could be ambiguous at distinguishing between changes in the two feature dimensions at the level of the single neuron in the context of this feature-attention task. Therefore, it could be advantageous for neurons to emphasize the temporal encoding of AM in this context in order to discriminate more precisely between the presence of AM changes and spectral content changes. Our second study presented here examines how amplitude modulation frequency discrimination changes when subjects are presented with bimodal audiovisual stimuli and switch between attending the auditory stimulus and attending the visual stimulus. Additionally, subjects are presented with unimodal trials in each modality, allowing for the comparison of AM encoding between unimodal and bimodal conditions. In both of these studies, we expect the encoding of AM to be stronger when the subjects are attending to it compared to when the subject should be ignoring changes in that dimension. Further, for the intermodal task, we would expect AM encoding to be better in the unimodal condition compared to when the animal is attending to the auditory stimulus in the presence of the distracting visual stimulus.

In addition to sensory processing, auditory cortex has been shown to have activity related to other task-relevant variables, such as reward expectation (Brosch et al. 2011; David et al. 2012; Guo et al. 2019), visual and somatosensory stimuli (Bizley and King 2009; Brosch 2005; Ghazanfar 2005; Kayser et al. 2005, 2008), and behavioral choice (Guo et al. 2019; Niwa et al. 2012b, 2013; Tsunada et al. 2016). However, it remains unclear what the function of this non-auditory activity is. For example, it remains debated whether choice-related activity in auditory cortex reflects a feedforward process of the sensory information informing the behavioral decision or whether it is resultant of feedback from other areas where the decision was made or where motor-planning is occurring. There has also been disparate evidence as to where choice-related activity may be found in auditory cortex with some studies not finding choice-related activity at all (Elgueda et al. 2019; Lemus et al. 2009; Tsunada et al. 2011), some finding it in higher level areas, but not primary auditory cortex (Christison-Lagay and Cohen 2018; Tsunada et al. 2016), and others finding it as early as primary auditory cortex (Atiani et al. 2014; Bathellier et al. 2012; Bizley et al. 2013; Huang et al. 2019; Niwa et al. 2012b).

In these studies, we aim to further investigate the nature of choice-related activity in auditory cortex. In both experiments, we utilize a two-alternative forced-choice task design, where subjects are required to make a movement to report either response, which will help to disentangle whether choice-related activity in auditory cortex is solely reflective of motor-preparatory activity. Further, in the intermodal attention experiment, on a subset of trials animals will be making perceptual judgements on visual stimuli in the absence of an auditory stimulus. We expect that if choice-related activity in auditory cortex is reflective of a feedforward transformation of sensory information into behavioral decisions, there would be an absence of choice-related activity during visual unimodal trials. However, if choice-related activity in auditory cortex is reflective of feedback processes, it is possible that choice-related activity would continue to be observed during visual unimodal trials. Taken together, these studies aim to advance our understanding of the mechanisms of attention in auditory cortex and how it may modulate both sensory encoding and decision-related activity.

References

Angeloni C, **Geffen M**. Contextual modulation of sound processing in the auditory cortex. *Current Opinion in Neurobiology* 49: 8–15, 2018.

Atiani S, **David SV**, **Elgueda D**, **Locastro M**, **Radtke-Schuller S**, **Shamma SA**, **Fritz JB**. Emergent Selectivity for Task-Relevant Stimuli in Higher-Order Auditory Cortex. *Neuron* 82: 486–499, 2014.

Bathellier B, **Ushakova L**, **Rumpel S**. Discrete Neocortical Dynamics Predict Behavioral Categorization of Sounds. *Neuron* 76: 435–449, 2012.

Benson DA, **Hienz RD**. Single-unit activity in the auditory cortex of monkeys selectively attending left vs. right ear stimuli. *Brain Research* 159: 307–320, 1978.

Bieser A, **Mueller-Preuss P**. Auditory responsive cortex in the squirrel monkey: neural responses to amplitude-modulated sounds. *Experimental Brain Research* 108, 1996.

Bizley JK, **King AJ**. Visual influences on ferret auditory cortex. *Hearing Research* 258: 55–63, 2009.

Bizley JK, **Walker KMM**, **Nodal FR**, **King AJ**, **Schnupp JWH**. Auditory Cortex Represents Both Pitch Judgments and the Corresponding Acoustic Cues. *Current Biology* 23: 620–625, 2013.

Bregman AS. *Auditory Scene Analysis: The Perceptual Organization of Sound*. MIT Press, 1994.

Brosch M. Nonauditory Events of a Behavioral Procedure Activate Auditory Cortex of Highly Trained Monkeys. *Journal of Neuroscience* 25: 6797–6806, 2005.

Brosch M, **Selezneva E**, **Scheich H**. Representation of Reward Feedback in Primate Auditory Cortex. *Frontiers in Systems Neuroscience* 5, 2011.

Buran BN, **von Trapp G**, **Sanes DH**. Behaviorally Gated Reduction of Spontaneous Discharge Can Improve Detection Thresholds in Auditory Cortex. *Journal of Neuroscience* 34: 4076–4081, 2014.

Carcea I, **Insanally MN**, **Froemke RC**. Dynamics of auditory cortical activity during behavioural engagement and auditory perception. *Nat Commun* 8: 14412, 2017.

Christison-Lagay KL, **Cohen YE**. The Contribution of Primary Auditory Cortex to Auditory Categorization in Behaving Monkeys. *Front Neurosci* 12: 601, 2018.

Cohen MR, **Maunsell JHR**. Attention improves performance primarily by reducing interneuronal correlations. *Nature Neuroscience* 12: 1594–1600, 2009.

Cohen MR, **Maunsell JHR**. Using Neuronal Populations to Study the Mechanisms Underlying Spatial and Feature Attention. *Neuron* 70: 1192–1204, 2011.

David SV, **Fritz JB**, **Shamma SA**. Task reward structure shapes rapid receptive field plasticity in auditory cortex. *Proceedings of the National Academy of Sciences* 109: 2144–2149, 2012.

Desimone R, **Duncan J**. Neural Mechanisms of Selective Visual Attention. *Annual Review of Neuroscience* 18: 193–222, 1995.

Downer JD, **Niwa M**, **Sutter ML**. Task Engagement Selectively Modulates Neural Correlations in Primary Auditory Cortex. *Journal of Neuroscience* 35: 7565–7574, 2015.

Downer JD, **Rapone B**, **Verhein J**, **O'Connor KN**, **Sutter ML**. Feature-Selective Attention Adaptively Shifts Noise Correlations in Primary Auditory Cortex. *The Journal of Neuroscience* 37: 5378–5392, 2017.

Elgueda D, **Duque D**, **Radtke-Schuller S**, **Yin P**, **David SV**, **Shamma SA**, **Fritz JB**. State-dependent encoding of sound and behavioral meaning in a tertiary region of the ferret auditory cortex. *Nat Neurosci* 22: 447–459, 2019.

Elliott TM, **Theunissen FE**. The Modulation Transfer Function for Speech Intelligibility. *PLoS Comput Biol* 5: e1000302, 2009.

Fritz J, **Shamma S**, **Elhilali M**, **Klein D**. Rapid task-related plasticity of spectrotemporal receptive fields in primary auditory cortex. *Nature Neuroscience* 6: 1216–1223, 2003.

Fritz JB. Differential Dynamic Plasticity of A1 Receptive Fields during Multiple Spectral Tasks. *Journal of Neuroscience* 25: 7623–7635, 2005.

Fritz JB, **Elhilali M**, **Shamma SA**. Adaptive Changes in Cortical Receptive Fields Induced by Attention to Complex Sounds. *Journal of Neurophysiology* 98: 2337–2346, 2007.

Gao X, **Wehr M**. A Coding Transformation for Temporally Structured Sounds within Auditory Cortical Neurons. *Neuron* 86: 292–303, 2015.

Gervain J, **Geffen MN**. Efficient Neural Coding in Auditory and Speech Perception. *Trends in Neurosciences* 42: 56–65, 2019.

Ghazanfar AA. Multisensory Integration of Dynamic Faces and Voices in Rhesus Monkey Auditory Cortex. *Journal of Neuroscience* 25: 5004–5012, 2005.

Grimault N, **Bacon SP**, **Micheyl C**. Auditory stream segregation on the basis of amplitude-modulation rate. *The Journal of the Acoustical Society of America* 111: 1340–1348, 2002.

Guo L, **Weems JT**, **Walker WI**, **Levichev A**, **Jaramillo S**. Choice-Selective Neurons in the Auditory Cortex and in Its Striatal Target Encode Reward Expectation. *J Neurosci* 39: 3687–3697, 2019.

Hocherman S, **Benson DA**, **Goldstein MH**, **Heffner HE**, **Hienz RD**. Evoked unit activity in auditory cortex of monkeys performing a selective attention task. *Brain Research* 117: 51–68, 1976.

Hoglen NEG, **Larimer P**, **Phillips EAK**, **Malone BJ**, **Hasenstaub AR**. Amplitude modulation coding in awake mice and squirrel monkeys. *Journal of Neurophysiology* 119: 1753–1766, 2018.

Huang Y, **Heil P**, **Brosch M**. Associations between sounds and actions in early auditory cortex of nonhuman primates. *eLife* 8: e43281, 2019.

Hubel DH, **Henson CO**, **Rupert A**, **Galambos R**. “Attention” Units in the Auditory Cortex. *Science, New Series* 129: 1279–1280, 1959.

Johnson JS, **Niwa M**, **O’Connor KN**, **Sutter ML**. Amplitude modulation encoding in the auditory cortex: comparisons between the primary and middle lateral belt regions. *Journal of Neurophysiology* 124: 1706–1726, 2020.

Johnson JS, **Yin P**, **O’Connor KN**, **Sutter ML**. Ability of primary auditory cortical neurons to detect amplitude modulation with rate and temporal codes: neurometric analysis. *Journal of Neurophysiology* 107: 3325–3341, 2012.

Joris PX, **Schreiner CE**, **Rees A**. Neural Processing of Amplitude-Modulated Sounds. *Physiological Reviews* 84: 541–577, 2004.

Kayser C, **Petkov CI**, **Augath M**, **Logothetis NK**. Integration of Touch and Sound in Auditory Cortex. *Neuron* 48: 373–384, 2005.

Kayser C, **Petkov CI**, **Logothetis NK**. Visual Modulation of Neurons in Auditory Cortex. *Cerebral Cortex* 18: 1560–1574, 2008.

Lee C-C, **Middlebrooks JC**. Auditory cortex spatial sensitivity sharpens during task performance. *Nature Neuroscience* 14: 108–114, 2011.

Lemus L, **Hernandez A**, **Romo R**. Neural codes for perceptual discrimination of acoustic flutter in the primate auditory cortex. *Proceedings of the National Academy of Sciences* 106: 9471–9476, 2009.

Malone BJ, **Beitel RE**, **Vollmer M**, **Heiser MA**, **Schreiner CE**. Modulation-Frequency-Specific Adaptation in Awake Auditory Cortex. *The Journal of Neuroscience* 35: 5904–5916, 2015.

Maunsell JHR. Neuronal Mechanisms of Visual Attention. *Annual Review of Vision Science* 1: 373–391, 2015.

Miller JM, **Sutton D**, **Pfingst B**, **Ryan A**, **Beaton R**, **Gourevitch G**. Single Cell Activity in the Auditory Cortex of Rhesus Monkeys: Behavioral Dependency. *Science, New Series* 177: 449–451, 1972.

Mirabella G, **Bertini G**, **Samengo I**, **Kilavik BE**, **Frilli D**, **Della Libera C**, **Chelazzi L**. Neurons in Area V4 of the Macaque Translate Attended Visual Features into Behaviorally Relevant Categories. *Neuron* 54: 303–318, 2007.

Niwa M, **Johnson JS**, **O’Connor KN**, **Sutter ML**. Active Engagement Improves Primary Auditory Cortical Neurons’ Ability to Discriminate Temporal Modulation. *Journal of Neuroscience* 32: 9323–9334, 2012a.

Niwa M, **Johnson JS**, **O’Connor KN**, **Sutter ML**. Activity Related to Perceptual Judgment and Action in Primary Auditory Cortex. *Journal of Neuroscience* 32: 3193–3210, 2012b.

Niwa M, **Johnson JS**, **O'Connor KN**, **Sutter ML**. Differences between Primary Auditory Cortex and Auditory Belt Related to Encoding and Choice for AM Sounds. *Journal of Neuroscience* 33: 8378–8395, 2013.

Niwa M, **O'Connor KN**, **Engall E**, **Johnson JS**, **Sutter ML**. Hierarchical effects of task engagement on amplitude modulation encoding in auditory cortex. *Journal of Neurophysiology* 113: 307–327, 2015.

O'Connell MN, **Barczak A**, **Schroeder CE**, **Lakatos P**. Layer Specific Sharpening of Frequency Tuning by Selective Attention in Primary Auditory Cortex. *The Journal of Neuroscience* 34: 16496–16508, 2014.

Osmanski MS, **Wang X**. Behavioral Dependence of Auditory Cortical Responses. *Brain Topogr* 28: 365–378, 2015.

Overton JA, **Recanzone GH**. Effects of aging on the response of single neurons to amplitude-modulated noise in primary auditory cortex of rhesus macaque. *Journal of Neurophysiology* 115: 2911–2923, 2016.

Rodgers CC, **DeWeese MR**. Neural Correlates of Task Switching in Prefrontal Cortex and Primary Auditory Cortex in a Novel Stimulus Selection Task for Rodents. *Neuron* 82: 1157–1170, 2014.

Schreiner CE, **Urbas JV**. Representation of amplitude modulation in the auditory cortex of the cat. II. Comparison between cortical fields. *Hearing Research* 32: 49–63, 1988.

Schwartz ZP, **David SV**. Focal Suppression of Distractor Sounds by Selective Attention in Auditory Cortex. *Cerebral Cortex* 28: 323–339, 2018.

Singh NC, **Theunissen FE**. Modulation spectra of natural sounds and ethological theories of auditory processing. *The Journal of the Acoustical Society of America* 114: 3394–3411, 2003.

Tsunada J, **Lee JH**, **Cohen YE**. Representation of speech categories in the primate auditory cortex. *Journal of Neurophysiology* 105: 2634–2646, 2011.

Tsunada J, **Liu ASK**, **Gold JI**, **Cohen YE**. Causal contribution of primate auditory cortex to auditory perceptual decision-making. *Nature Neuroscience* 19: 135–142, 2016.

Wimmer RD, **Schmitt LI**, **Davidson TJ**, **Nakajima M**, **Deisseroth K**, **Halassa MM**. Thalamic control of sensory selection in divided attention. *Nature* 526: 705–709, 2015.

Yin P, **Johnson JS**, **O'Connor KN**, **Sutter ML**. Coding of Amplitude Modulation in Primary Auditory Cortex. *Journal of Neurophysiology* 105: 582–600, 2011.

Chapter 1

Choice-related activity and neural encoding in primary auditory cortex and lateral belt during feature selective attention

Abstract

Selective attention is necessary to sift through, form a coherent percept of, and make behavioral decisions on the vast amount of information present in most sensory environments. How and where selective attention is employed in cortex and how this perceptual information then informs the relevant behavioral decisions is still not well understood. Studies probing selective attention and decision making in visual cortex have been enlightening as to how sensory attention might work in that modality; whether or not similar mechanisms are employed in auditory attention is not yet clear. Therefore, we trained rhesus macaques on a feature selective attention task, where they switched between reporting changes in temporal (amplitude modulation, AM) and spectral (carrier bandwidth) features of a broadband noise stimulus. We investigated how the encoding of these features by single neurons in primary (A1) and secondary (middle lateral belt, ML) auditory cortex were affected by the different attention conditions. We found that neurons in A1 and ML showed mixed-selectivity to the sound and task features. We found no difference in AM encoding between the attention conditions. We found that choice-related activity in both A1 and ML neurons shifts between attentional conditions. This finding suggests that choice-related activity in auditory cortex does not simply reflect motor preparation or action, and supports the relationship between reported choice-related activity and the decision and perceptual process.

Introduction

The auditory system is often faced with the difficult challenge of encoding a specific sound in a noisy environment, such as following a conversation in a loud room. The neural mechanisms by which the auditory system attends to one sound source and ignores distracting sounds are not yet understood. Studies probing the mechanisms underlying auditory attention in cortex have been largely concerned with task engagement, wherein the effects of active performance on neural activity are compared to those of passive listening. Studies in auditory cortex (AC) utilizing this paradigm have shown that task engagement can improve behaviorally-relevant neural sound discrimination (Atiani et al. 2014; Bagur et al. 2018; Buran et al. 2014; Carcea et al. 2017; Francis et al. 2018a; Niwa et al. 2012a, 2015; von Trapp et al. 2016), modulate neuronal tuning (Fritz et al. 2003, 2007; Fritz 2005; Lee and Middlebrooks 2011; Lin et al. 2019; Yin et al. 2014), alter the structure of correlated variability within neural populations (Downer et al. 2015, 2017a), as well as other effects (Massoudi et al. 2014; Angeloni and Geffen 2018; Osmanski and Wang 2015; Sutter and Shamma 2011). Though informative, this active/passive paradigm makes it difficult to disentangle arousal and motor effects from the mechanisms more specifically employed in selectively attending to a single sound source or feature amidst auditory ‘clutter’.

Studies on the neural basis of auditory selective attention at the single neuron level are rare (Schwartz and David 2018), and non-spatial auditory feature-selective attention has been relatively unexplored (Downer et al. 2017b). Feature-selective attention, which segregates particular sound features, such as intensity or fundamental frequency, is essential for tasks such as discriminating between talkers in a noisy environment (Bregman 1994; McDermott 2009; Bizley and Cohen 2013; Shinn-Cunningham 2008; Woods and McDermott 2015). Furthermore, it can prove useful for listeners to switch between attended sound features because the most distinctive feature dimensions may vary across sources (Woods and McDermott 2015; Bregman 1994).

In visual cortex, feature-based attention has been suggested to follow a gain model similar to spatial attention, where responsivity to the attended feature increases in cells tuned to the attended feature and decreases in cells tuned to orthogonal features (Martinez-Trujillo and Treue 2004; Maunsell and Treue 2006). Studies of spatial attention in AC single neurons suggest that AC employs a mechanism similar to that reported in visual cortex, where a gain in neural activity increases when attention is directed into the receptive field of a neuron and, conversely, gain decreases when attention is directed outside the receptive field (Engle and Recanzone 2013; Lee and Middlebrooks 2011; Scott et al. 2007) . We endeavored to see if feature-selective attention in AC is also facilitated by a gain in activity in neurons tuned to an attended feature.

How and where task relevant sensory information is transformed into a decision in the brain is still largely unclear. Reports of activity correlated to the reported decision in AC have been mixed where some have not found choice-related activity (Elgueda et al. 2019; Lemus et al. 2009; Tsunada et al. 2011), some have found it in higher areas, but not A1 (Christison-Lagay et al. 2017; Tsunada et al. 2016), and some studies have found it as early as primary auditory cortex (A1) (Atiani et al. 2014; Bathellier et al. 2012; Bizley et al. 2013; Christison-Lagay et al. 2017; Christison-Lagay and Cohen 2018; Francis et al. 2018b, 2018b; Gronskaya and von der Behrens 2019; Guo et al. 2019; Huang et al. 2019; Niwa et al. 2012b; Runyan et al. 2017). As one progresses further along the auditory cortical hierarchy, there is either an increasingly larger proportion of neurons showing activity correlated to the decision, or the nature of the choice signal changes (Atiani et al. 2014; Niwa et al. 2013; Tsunada et al. 2016). Both cases suggest that the sensory evidence informing task-relevant decisions is transformed as the information moves up the processing stream (Bizley and Cohen 2013; Hackett 2011; Huang and Brosch 2020; Romanski et al. 1999).

There has also been uncertainty as to whether the reported choice activity in AC could be more reflective of motor influences than perceptual or decision-related influences. Go/No-Go tasks are typically used in auditory cortical studies, and these tasks require movement for report of one choice, but not the other (Brosch 2005; Niwa et al. 2013); forced-choice tasks reduce this uncertainty by requiring movements for either report (Guo et al. 2019). It has been well documented that movement can modulate auditory cortical activity (Eliades and Wang 2003; Guo et al. 2019; Schneider et al. 2014). Here, we employ a Yes/No forced-choice task format in which a movement is required for both responses in order to disentangle motor-related from choice-related activity in AC.

We investigated whether a mechanism for feature-selective attention similar to feature-based attention in visual cortex is employed in primary (A1) and secondary (middle lateral belt, ML) auditory cortex using noise that was amplitude modulated (AM) or bandwidth restricted (∆BW). Monkeys were presented sounds that varied either in spectral (∆BW) or temporal (AM) dimensions, or both, and performed a detection task in which they reported change along one of these feature dimensions. In this study, we focus on the amplitude modulation feature, as it has been well studied and is a salient communicative sound feature for humans and other animals (Schnupp 2006; Shannon et al. 1995; Van Tasell et al. 1987; Wang et al. 2007) and can be helpful in sound source segregation (Bregman 1994; Grimault et al. 2002). Spectral content changes were used as a difficulty-matched attentional control. We hypothesized we would see a gain in AM encoding when animals were cued to attend to that feature, compared to when they were cued to attend ∆BW changes. We also examined choice-related activity in AC, hypothesizing to find a larger proportion of neurons with significant choice-related activity in higher-order AC (ML) than in A1.

Materials and Methods

Subjects.

Subjects were two adult rhesus macaques, one male (13kg, 14-16 years old), one female (7kg, 17-19 years old). All animals were fluid regulated and all procedures were approved by the University of California–Davis Animal Care and Use Committee and met the requirements of the United States Public Health Service policy on experimental animal care.

Stimuli.

Stimuli were constructed from broadband Gaussian (white) noise bursts (400 ms; 5 ms cosine ramped), 9 octaves in width (40 to 20480 Hz). Four different seeds were used to create the carrier noise, which was frozen across trials. To introduce variance along spectral and temporal dimensions, the spectral bandwidth of the noise was narrowed (∆BW) and/or the noise envelope was sinusoidally amplitude modulated (AM). The extent of variation in each dimension was manipulated to measure behavioral and neural responses above and below threshold for detecting each feature.

Sound generation methods have been previously reported (O’Connor et al., 2011). Briefly, sound signals were produced using an in-house MATLAB program and a digital-to-analog converter (Cambridge Electronic Design [CED] model 1401). Signals were attenuated (TDT Systems PA5, Leader LAT-45), amplified (RadioShack MPA-200), and presented from a single speaker (RadioShack PA-110) positioned approximately 1.5 m in front of the subject centered at the interaural midpoint. Sounds were generated at a 100 kHz sampling rate. Intensity was calibrated across all sounds (Bruel & Kjaer model 2231) to 65 dB at the outer ear. It is important to note that some methods of generating ∆BW introduce variation in that sound's envelope, however we implemented a synthesis method that constructs noise using a single-frequency additive technique and thus avoids introducing envelope variations that could serve as cues for ∆BW (Strickland and Viemeister 1997).

Recording procedures.

Each animal was implanted with a head post centrally behind the brow ridge and a recording cylinder over an 18 mm craniotomy over the left parietal lobe using aseptic surgical techniques (O'Connor et al. 2005). Placement of the craniotomy was based on stereotactic coordinates of auditory cortex to allow vertical access through parietal cortex to the superior temporal plane (Saleem and Logothetis 2007).

All recordings took place in a sound attenuating, foam-lined booth (IAC: 2.9x3.2x2 meters) while subjects sat in an acoustically transparent chair (Crist Instruments). Three quartz-coated tungsten microelectrodes (Thomas Recording, 1–2 MΩ; 0.35 mm horizontal spacing; variable, independently manipulated vertical spacing) were advanced vertically to the superior surface of the temporal lobe. Extracellular signals were amplified (AM Systems model 1800), bandpass filtered between 0.3 Hz and 10 kHz (Krohn-Hite 3382), and then converted to a digital signal at a 50 kHz sampling rate (CED model 1401). During electrode advancement, auditory responsive neurons were isolated by presenting various sounds while the subject sat passively. When at least one auditory responsive single unit was well isolated, we measured neural responses to the two features while the subjects sat passively awake. At least 10 repetitions of each of the following stimuli were presented: the unmodulated noise, each level of bandwidth restriction, and each of the possible AM test modulation frequencies (described below). We also measured pure tone tuning and responses to bandpass noise to aid in distinguishing area boundaries.

After completing these measures, experimental behavioral testing and recording began. When possible, tuning responses to the tested stimuli were again measured after task performance, to ensure stability of electrodes throughout the recording. Contributions of single units (SUs) to the signal were determined offline using principal components analysis-based spike sorting tools from Spike2 (CED). Single unit waveform templates were generated using Spike2's template forming algorithms, and spikes were assigned to matching templates. Single units were confirmed by their separability in principal-component space. Spiking activity was generally 4–5 times the visually assessed background noise level. Fewer than 0.1% of spike events assigned to single unit clusters fell within a 1 ms refractory period window. Only recordings in which neurons were well isolated for at least 180 trials within each condition were included in analysis here.

Cortical field assessment.

Recording locations were determined using both stereotactic coordinates (Martin and Bowden 1996) and established physiological measures (Merzenich and Brugge 1973; Rauschecker and Tian 2000; Tian and Rauschecker 2004). In each animal, we mapped characteristic frequency (CF) and preference between pure tones and bandpass noise to establish a topographic distribution of each (Figure 1.1). Tonotopic gradient reversal, BW distribution, spike latency and response robustness to pure tones was used to estimate the boundary between A1 and ML and assign single units to an area (Downer et al. 2017a; Niwa et al. 2015). Recordings were assigned to their putative cortical fields *post hoc* using recording location, tuning preferences, and latencies.

Feature attention task.

This feature attention task has been previously described in detail (Downer et al. 2017b). The subjects performed a change detection task in which only changes in the attended feature were relevant for the task. Subjects moved a joystick laterally to initiate a trial, wherein an initial sound (the S1, always the 9-octave-wide broadband, unmodulated noise) was presented, followed by a second sound (S2) after a 400ms inter-stimulus interval (ISI). The S2 could be identical to the S1, it could change by being amplitude-modulated (AM), it could change by being bandwidth restricted (∆BW), or it could change along both feature dimensions.

Only three values of each feature (AM, ∆BW) were presented, limiting the size of the stimulus set in order to obtain a reasonable number of trials for each stimulus under each attention condition to compare in analyses. The stimulus space was further reduced by presenting only a subset of the possible co-varying stimuli. Within each recording session, we presented 13 total stimuli. To equilibrate difficulty between the two features, we presented values of each feature so that one was near each animal's behavioral threshold of detection, one was slightly above, and one far above threshold.

Thresholds were determined for each feature and subject independently using six levels of each feature before choosing three values and beginning the co-varying feature attention task. For Monkey U, the ∆BW values were 0.375, 0.5, and 1 octave and the AM depth values were 28%, 40%, and 100%. For Monkey W, the ∆BW values were 0.5, 0.75, and 1.5 octaves and the AM depth values were 40%, 60%, and 100%. For all analyses in which data are collapsed across subjects, ∆BW values and AM values are presented as ranks (∆BW 0-3 and AM 0-3) . Each animal's behavioral performance during feature attention was similar at these values. For AM 1 they were slightly above chance (Monkey W 53% correct, Monkey U 59%), for AM2 they were better (Monkey W 71% correct, monkey U 75% correct) and they were quite good at detecting AM3 (Monkey W 86% correct, Monkey U 89% correct). Performance was similar for increasing values of ∆BW where Monkey W performed at 54%, 73% and 90% correct, and Monkey U performed at 65%, 76% and 88% correct for ∆BW 1-3 respectively. Performance was calculated for each session with a regression model (Downer et al. 2017b) which showed that in general the monkeys were performing the task using the appropriate feature (Figure 1.2a). There was also no systematic relationship of performance drifts with early or late trials within a session or block (Figure 1.2bc). Behavior from the A1 sessions have been previously reported in more detail (Downer et al. 2017b) and performance was similar during the ML recording sessions.

Within a given session, AM sounds were presented at only a single modulation frequency. Across sessions, a small set of frequencies was used (15, 22, 30, 48, and 60 Hz). The AM frequency was selected randomly each day. Subjects were cued visually via an LED above the speaker as to which feature to attend (green or red light, counterbalanced between subjects). Additionally, before each block of feature attention trials, there was a 60-trial instruction block in which the S2s presented were only altered along the target feature dimension (i.e., sounds containing the distractor feature were not presented). Subjects were to respond with a “yes” (up or down joystick movement, counterbalanced across subjects) on any trial in which the attended feature was presented, otherwise, the correct response was “no” (opposite joystick movement). We chose upward or downward joystick movement to avoid influences on single neuron choice activity dependent on contralateral movements. Such movement related activity has been recently reported in other studies (Guo et al. 2019). Hits and correct rejections were rewarded with a drop of water or juice and misses and false alarms resulted in a penalty (3–5 s timeout).

During the test conditions, the S2 was unmodulated broadband noise (no change from S1) on 25% of the trials, co-varying on 25% of the trials, and contained only ∆BW or AM on 25% of the trials respectively. Sounds in the set were presented pseudo-randomly such that, over sets of 96 trials, the entire stimulus set was presented exhaustively (including all four random noise seeds). Block length was variable, based in part on subjects’ performance, to ensure a sufficient number of correct trials for each stimulus. Not including instruction trials, block length was at least 180 trials and at most 360 trials, to ensure that subjects performed in each attention condition at least once during the experiment. Subjects could perform each attention condition multiple times within a session. Only sessions in which subjects completed at least 180 trials per condition (excluding instruction trials) were considered for analysis in this study.

Analysis of single neuron feature selectivity

Spike counts (SC) were calculated over the entire 400ms stimulus window. SCs in response to feature-present stimuli were normalized over the entire spike count distribution across both features, including unmodulated noise, for that cell. To characterize this response function, we calculated a feature-selectivity index (FSI) for each feature as follows:

[1]
$$FSI_{AM} = \frac{SC_{AM_{>0},\Delta BW_0} - SC_{AM_0,\Delta BW_0}}{SC_{AM_{>0},\Delta BW_0} + SC_{AM_0,\Delta BW_0}}$$

[2]
$$FSI_{BW} = \frac{SC_{\Delta BW_{>0},\mathrm{AM}_0} - SC_{\Delta BW_0,AM_0}}{SC_{\Delta BW_{>0},AM_0} + SC_{\Delta BW_0,AM_0}}$$

Where SC_x is the mean SC in response to the given set of stimuli designated by the subscript. A Kruskal–Wallis rank-sum test was performed between distributions of SCs with the feature-present (feature level greater than 0) and those with the feature-absent (feature value of 0) to determine the significance of the FSI for each neuron. Cells that had a significant FSI for a given feature were categorized as encoding that feature with firing rate. Neurons were classified as having ‘increasing’ (or ‘decreasing’) responses to a feature if their FSI was greater than (or less than) zero for that feature.

Phase projected vector strength

Vector strength (VS) is a metric that describes the degree to which the neural response is phase-locked to the stimulus (Goldberg and Brown 1969; Mardia and Jupp 2000). VS is defined as:

[3] $$VS = \frac{\sqrt{(\sum_{i=1}^{n} \cos \theta_i)^2 + (\sum_{i=1}^{n} \sin \theta_i)^2}}{n}$$

Where *n* is the number of spikes over all trials and θ_i is the phase of each spike, in radians, calculated by:

[4] $$\theta_i = 2\pi \frac{t_{i \, mod \, p}}{p}$$

Where t_i is the time of the spike (in ms) relative to the onset of the stimulus and *p* is the modulation period of the stimulus (in ms). When spike count is low, VS tends to be spuriously high. Phase projected Vector Strength (VS_{pp}), is a variation on VS developed to help mitigate issues with low SC trials (Yin et al. 2011). VS_{pp} is calculated by first calculating VS for each trial, then comparing the mean phase angle of each trial to the mean phase angle of all trials. The trial VS value is penalized if out of phase with the global mean response. VS_{pp} is defined as:

[5] $$VS_{pp} = VS_t \cos(\phi_t - \phi_c)$$

Where VS_{pp} is the phase-projected vector strength per trial, VS_t is the vector strength per trial, as calculated in [1], and φ_t and φ_c are the trial-by-trial and mean phase angle in radians, respectively, calculated for each stimulus by:

[6] $$\phi = arctan2\left(\frac{\sum_{i=1}^{n} \sin \theta_i}{\sum_{i=1}^{n} \cos \theta_i}\right)$$

Where *n* is the number of spikes per trial (for φ_t) or across all trials (for φ_c). In this report, we use VS_{pp} exclusively to measure phase-locking, as SC tended to be relatively low and VS and VS_{pp} tend to be in good agreement with the exception of low SCs where VS_{pp} tends to be more accurate than VS (Yin et al.

2011). To determine significance of VS_{pp} encoding for each neuron, a Kruskal–Wallis rank-sum test was preformed between distributions of VS_{pp} values on trials with non-zero AM depths, to those from unmodulated noise trials. Of note, VS_{pp} in response to an unmodulated stimulus, is a control measurement assuming the same modulation frequency as the corresponding AM frequency from that recording session.

Analysis of neural discriminability

We applied the area under the receiver operating characteristic (ROCa), a signal detection theory-based (Green and Swets 1974), to measure how well neurons could detect each feature. ROCa represents the probability an ideal observer can detect the presence of the target feature given only a measure of the neural responses (either firing rate or VS_{pp}). To calculate ROCa, we partitioned the trial-by-trial neural responses into two distributions: those when the target feature was present in the stimulus and trials where it was absent. Then we determined the proportion of trials in each group where the neural response exceeds a criterion value. We repeated the measure using 100 criterion values, covering the whole range of responses. The graph of the probability of exceeding the criterion for feature-present trials (neural 'hits') versus the probability of exceeding the criterion for feature-absent trials (neural false alarms) plotted for all 100 criteria as separate points creates the ROC. The area under this curve is the ROCa. ROCa is bounded by 0 and 1, where both extremes indicate perfect discrimination between target feature-present and -absent stimuli, and 0.5 indicates a chance level of discrimination between the two distributions.

Analysis of choice-related activity

Choice probability (CP) is an application of ROC analysis used to measure the difference between neural responses contingent on what the animal reports, for example, whether a stimulus feature is present or absent (Britten et al. 1992, 1996). Similar to ROCa described above, CP values are bounded by 0 and 1, and a CP value of 0.5 indicates no difference (or perfect overlap) in the neural responses between 'feature-present' and 'feature-absent' reports. A CP value of 1 means for every trial that the animal reports a feature, the neuron fired more than on trials where the animal did not report the feature.

A CP value of 0 means that, for every trial that the animal reports a feature, the neuron fired *less* than on trials where the animal did not report the feature. Stimuli that did not have at least 5 'yes' and 5 'no' responses were excluded from analyses. CP was calculated based on both firing rate and on VS_{pp}. For rate-based CP, we calculated CP both for each stimulus separately, and pooled across stimuli. We calculated this stimulus-pooled CP by first separating the 'yes' and 'no' response trials within stimulus, then converting these rates into z-scores within a stimulus, then combined these z-scored responses across stimuli. This type of z-scoring has been found to be conservative in estimating CP (Kang and Maunsell 2012). CP was calculated during both the 400ms stimulus presentation (S2) and during the response window (RW), the time after stimulus offset and prior to the response (typically ~0.2 – 3.0s). The significance of each neuron's CP was determined using a permutation test (Britten et al. 1996). The neural responses were pooled between the 'feature-present report' and 'feature-absent report' distributions and random samples were taken (without replacement). CP was then calculated from this randomly sampled set. This procedure was repeated 2000 times. The *p* value is the proportion of CP values from these randomly sampled repeats that were greater than the CP value from the non-shuffled distributions.

Results

We recorded activity from 92 single units in A1 (57 from Monkey W, 35 from Monkey U) from 16 recording sessions and 122 single units in ML (49 from Monkey W, 73 from Monkey U) over 17 recording sessions as animals performed a feature-selective attention task. All metrics reported here were first assessed separately for each subject and were determined to be similar between the animals (Wilcoxon rank sum test >0.05) and thus were pooled to increase our statistical power.

The raster plots of neural activity are shown for three example neurons across different conditions for entire trials (Figure 1.3), and for the same neurons expanded just to show the responses to S2 (Figures 1.4, 1.5 and 1.6). Each neuron's ability to encode AM with firing rate or VSpp and/or to encode ∆BW is shown in the legend of Figure 1.3. In the examples from Figures 1.3, 1.4, 1.5, and 1.6, with one exception, when collapsing across ∆BW, for all AM stimuli (AM1,2,3) including unmodulated (AM0), the firing rate was higher in the attend-AM condition than attend ∆BW (Figures 1.4, 1.5 and 1.6, sub-panels).

The exception was AM3 in Figure 1.4. The example neurons in figures 1.4, 1.5 and 1.6 all monotonically increase firing rate as AM depth goes from level 1 to level 3, although the neuron in Figure 1.4 also responds strongly to the unmodulated noise (AM level 0). Also note that the neuron in Figure 1.4 shows strong phase-locking to AM. This overall effect was consistent with a population effect (later described in Figure 1.8) where, on average, there was a non-significant increase in firing rate across all stimuli in the attend AM condition, but because AM0 also increases this did not lead to increased neuronal ability to detect AM.

Feature tuning

There was no significant difference in the proportions of neurons in A1 and ML that encoded AM (47.8% A1, 38.5% ML; $p = 0.08$, $\chi 2$ test). We found a large proportion of neurons in both A1 and ML that were sensitive to the relatively small changes in ∆BW from the 9-octave wide unmodulated noise (Figure 1.7), though there was no difference in the proportion of ∆BW encoding neurons between areas (32.6% A1, 29.5% ML; $p = 0.18$, $\chi 2$ test; Table 1.1).

There was a positive correlation between AM and ∆BW selectivity in both A1 (Figure 1.7a, Pearson rho = 0.31, $p = 0.002$) and ML (Figure 1.7b, Pearson rho = 0.31, $p = 5.32$ e-4), so cells that tended to increase firing rate for increasing AM levels, also tended to increase firing rate for increasing ∆BW levels (FSI_{AM} vs. FSI_{BW}). In this feature selective attention task, we found no significant difference between A1 and ML in the proportions of 'increasing' and 'decreasing' encoding cells for either AM ('Increasing' $p = 0.21$ χ^2 test; 'Decreasing' $p = 0.11$ χ^2 test) or ∆BW ('Increasing' $p = 0.22$ χ^2 test; 'Decreasing' $p = 0.52$ χ^2 test).

A large population of neurons decreased firing rate for increasing AM depth ('decreasing cells') in both A1 and ML (Table 1.1, Figure 1.8cd). We also found that nearly half of the neurons in both A1 and ML decreased firing rate for increasing ∆BW (Table 1.1, Figure 1.9cd). However, the population of neurons that *significantly* encoded AM was largely dominated by cells that increased firing rate for increasing AM depth in both A1 and ML (Figure 1.8ab), with only 13.6% of AM encoders (6 cells, 6.5% of *all* A1 units) classified as 'decreasing' units in A1, and 10.6% of AM encoders 'decreasing' in ML (5 cells 4.1% of *all* ML units). Among significant ∆BW encoders, the population was more evenly split between ‘increasing’ and ‘decreasing’ units in both A1 and ML (Figure 1.9ab): 43.3% of ∆BW encoders (14.1% of *all* A1 units) have ‘decreasing’ functions in A1 vs. 30.6% in ML (9.0% of *all* ML units).

Vector strength encoding

We found a similar proportion of cells in A1 and ML that significantly phase-locked to AM ($p = 0.77$, χ^2 test), as measured by phase-projected vector strength (VS_{pp}) (Table 1.1). As in previous reports (Niwa et al. 2013), we found VS_{pp} to be weaker in ML than A1 at low AM depths (Figure 1.10cd, $p < 0.05$ at low AM depths, Wilcoxon rank-sum Test), but not significantly different at the highest AM depth ($p = 0.73$, Wilcoxon rank-sum test). In both A1 and ML, there was no significant difference in phase-locking (VS_{pp}) between the attend AM and attend ∆BW conditions ($p > 0.05$, signed-rank test, Figure 1.10cd).

Feature discriminability and context effects

We used the signal detection theory-based area under the receiver operating characteristic (ROCa) to measure how well an ideal observer could detect the presence of each sound feature based on the neural responses (either firing rate or VS_{pp}). Increases in the levels of both features tended to yield increasing ROCa (A1 AM Spearman rho = 0.15, ∆BW Spearman rho = .06; ML AM Spearman rho = 0.13, ∆BW Spearman rho = 0.05 (Figure 1.11). However, there was no significant effect of attentional condition on either feature at any level of feature modulation for either A1 (Figure 1.8a, 1.9a) or ML (Figure 1.8b, 1.9b).

VS_{pp} -based discrimination (ROCa) of AM from unmodulated sounds was better at the lowest modulation depth in A1 than in ML ($p = 0.02$, Wilcoxon Rank Sum Test, Figure 1.10ab). At the higher modulation depths, VS_{pp} -based discrimination was similar in A1 and ML ($p = 0.99$ AM depth 2; $p = 0.26$, AM depth 3; Wilcoxon Rank Sum Test; Figure 1.10ab). However, there was no significant difference in VS_{pp} discriminability between attention conditions for any modulation depth in either area ($p > 0.05$, signed-rank test, Figure 1.10ab).

Choice-related activity

In *A1*, during the attend AM condition, CP values were evenly distributed about 0.5 during the ISI (ISI median = 0.49, p = 0.11 signed-rank test), the stimulus presentation (S2 median CP = 0.50, p = 0.87 signed-rank test) and the response window (RW median CP = 0.49, p = 0.43 signed-rank test; Figure 1.12ace). In contrast, during the attend ΔBW context, the CP values tended to be lower than 0.5 during both the stimulus (S2 median CP = 0.49, p = 0.02 signed-rank test) and the response window (RW median CP =0.46, p = 4.2 e-8 signed-rank test), but not significantly different from 0.5 during the ISI (ISI median = 0.51, p = 0.92; Figure 1.12bdf). That is, during the attend ΔBW condition, the population of neurons tended to decrease firing rate when reporting target feature detection, whereas during the attend AM condition, it was equally likely for a neuron to increase firing rate for a report of target detection as it was for a report of target absence. There was a significant difference in the population CP distributions between attention conditions during the RW (Attend AM median = 0.49, Attend ΔBW median = 0.46, p = 0.004, signed-rank test), though neither during the ISI (p=0.33, signed-rank test) nor the S2 (p = 0.06, signed-rank test).

The choice-related activity in ML was similar to that reported above in A1 during the ISI and S2. During the attend AM condition, activity was evenly distributed about 0.5 (ISI median CP = 0.50, p = 0.47; S2 median CP = 0.50, p = 0.94, signed-rank test; Figure 1.13ac). During the attend ΔBW condition, average CP was less than 0.5 during the S2(S2 median CP = 0.49, p = 0.043 signed-rank test; Figure 1.13d), but not during the ISI (ISI median CP = 0.49, p = 0.15, signed-rank test; Figure 1.13b). However, during the response window, CP values were less than 0.5 in both the attend AM condition (median CP = 0.48, p = 0.004 signed-rank test) and the attend ΔBW condition (median CP = 0.47, p = 2.7 e-5 signed-rank test; Figure 1.13ef). This is in contrast to A1 where CP values tended to be lower than 0.5 only in the attend ΔBW condition. There was no significant difference in the distribution of CP values in ML neurons between the attend AM and attend ΔBW conditions during either the ISI (p = 0.49, signed-rank test) or the S2 (p = 0.15, signed-rank test). However, there was a significant difference in the CP distribution between the attend AM and attend ΔBW conditions in ML during the response window (Attend AM median = 0.48, Attend ΔBW median = 0.47, p = 0.033 signed-rank test), reflecting the population shift to CP values less than 0.5 in the attend ΔBW condition compared to the attend AM condition.

There was no significant difference in the proportion of neurons in A1 (19.5%) and ML (26.2%) with significant choice-related activity during the stimulus window ($p = 0.31$, χ2 test; Figures 1.12cd, 1.13cd), or ISI window (A1 17.4%, ML 20.5%, $p = 0.38$ χ2 test; Figures 1.12ab, 1.13ab). In both areas, the population of neurons with significant choice-related activity during the response window (from S2 end to joystick movement) was not significantly different between the two areas (41.3% A1, 34.4% ML, $p = 0.41$, χ2 test; Figures 1.12ef, 1.13ef). Additionally, the proportion of neurons with significant CP was larger during the response window than during both the ISI and the stimulus window.

Discussion

We found a large proportion of cells in ML that decreased firing rate with increasing AM detectability, similar to previous findings in ML (Johnson et al. 2020; Niwa et al. 2013). However, unlike these previous studies where ML had a significantly larger population of cells with decreasing AM depth functions than A1, we found a similar proportion of A1 neurons with decreasing AM depth functions. Further, the majority of neurons in both A1 and ML significantly encoding AM depth had increasing AM depth functions. This suggests that the encoding of amplitude modulation can be flexible depending upon the behavioral and sensory demands of the task. In essence, with increased perceptual difficulty, stimulus/feature ambiguity, and task difficulty it may be necessary for A1 to develop a more robust and appropriate code in order to solve the task, and for ML to take on more of the sensory processing, and thus the encoding schemes look more similar between these two areas.

We also found a large population of cells in both A1 and ML that were sensitive to changes in bandwidth. This was particularly surprising as the changes in bandwidth were relatively small compared to the 9-octave wide unmodulated noise. It's possible that the ∆BW encoding we saw was due to an increasing concentration of power in the middle frequencies of the broadband noise as the level of bandwidth restriction increased. It could also be caused by decreasing power in flanking inhibitory bands. Further studies investigating if and how neurons in A1 and ML encode small changes in spectral bandwidth to broad-band sounds under power-matched conditions could be enlightening.

Using phase-projected vector strength (VS_{pp}) as a measure of temporal coding, neither ML nor A1 single neurons showed attention-related changes in VS_{pp}-based sensitivity to AM or VS-based choice-related activity. This is consistent with previous results from our lab showing smaller effects for VS_{pp}-based attention and choice than for firing rate (Niwa et al. 2013). A recent study that could help interpretation of this result shows thalamic projections to the striatum (an area involved in decisions and possibly attention) relay information about temporally modulated sounds in the form of phase-locking, whereas cortical projections to the striatum only convey information about temporally modulated sounds with average firing rate over the stimulus (Ponvert and Jaramillo 2019).

Attending to the target-feature did not significantly improve single neuron amplitude modulation or bandwidth restriction detection in A1 or ML. This seems surprising considering the wide array of effects that have been previously reported in auditory cortex related to different tasks, and behavioral contexts (Atiani et al. 2014; Bagur et al. 2018; Buran et al. 2014; Francis et al. 2018a; Niwa et al. 2012b; Otazu et al. 2009; Lakatos et al. 2013; Angeloni and Geffen 2018; Sutter and Shamma 2011). In macaque monkeys, an improvement in both rate-based and temporal AM encoding was observed in A1 and ML neurons when animals performed a single-feature AM detection task compared to when animals passively listened to the same stimuli (Niwa et al. 2013, 2015). We did not see a similar level of encoding improvement, possibly due to the more fine-tuned form of attention needed to perform this task.

One might expect to observe smaller effects from this more selective form of attention than in a passive versus active listening task, as the difference between attending to one feature of a sound compared to another is much smaller than switching between paying attention to a sound and passive sound presentation. Furthermore, arousal, as measured with pupillometry, has recently been shown to correlate with increases in activity, gain and trial-to-trial reliability of A1 neurons (Schwartz et al. 2019), which could account for some of the effects seen in task engagement paradigms.

Feature-based attention has been shown to have gain effects on neurons tuned to the attended feature in visual cortex (Ni and Maunsell 2019; Treue and Trujillo 1999). It is possible that we did not see a similar gain effect of feature attention in AC due to the mixed-selectivity we and others (Chambers et al. 2014) found in the encoding of these features (i.e. most neurons are sensitive to both AM and ΔBW). However, it is likely that mixed-selectivity is not the only reason we did not see a gain effect. In a study where rats performed a frequency categorization task with shifting boundaries, Jaramillo and colleagues similarly found that neurons in AC did not improve their discriminability with attentional context (Jaramillo et al. 2014). This similar lack of enhancement seen in a task where only a single feature is modulated, suggests that the mechanism for feature attention in auditory cortex could be enacted via a different mechanism.

In visual cortical studies probing *selective* feature attention – where the subject must distinguish between features within a single object, rather than object- or place-oriented, feature-based attention – results have been similarly complex. At the level of the single neuron, there have not been clear, gain-like improvements in the sensitivity to the attended feature (Chen et al. 2012; Mirabella et al. 2007; Sasaki and Uka 2009; Uka et al. 2012). Further, the effects of feature-selective attention seem to be dependent upon not just the tuning preferences of a neuron, but also the strength of its tuning (Ruff and Born 2015). These studies, along with our own, suggest that segregation of features within an object may require a different mechanism relative to object-directed, feature-based attention.

In each of the feature-selective attention studies cited above, a common observation is that single neurons in sensory cortex have mixed selectivity for the features in the task, as opposed to being uniquely responsive to one feature or another. Such mixed selectivity among single neurons may permit sophisticated, flexible computations at the population level (Fusi et al. 2016). It thus seems likely the mechanism for feature-selective attention lies not at the level of the single neuron, but rather requires the integration of activity from a larger population of neurons. A feature-selective study using ERPs found that the neural responses to identical stimuli varied when the subjects attend to different features of the stimulus (Nobre et al. 2006). The single neuron and neural circuit mechanisms underlying this effect remain unclear. One such possible mechanism might be the structure of correlated variability within the population, which has been shown to be modulated by feature-selective attention (Downer et al. 2017b). Another study, simulating populations by pooling single-neurons across A1 recordings permitted clear segregation of these two features, as well as an enhancement in discrimination of the attended feature (Downer et al. 2020). Further studies investigating feature-selective attention at the level of populations of neurons are necessary to better understand the underlying mechanisms.

We did see an interesting difference in the distribution of choice-related activity between the attentional conditions, where the correlation between firing rate and choice shifted direction between conditions. During the attend AM context, CP was evenly distributed about 0.5 with some neurons showing significant choice activity at either extreme. In contrast, during the attend ∆BW context, CP values were shifted towards 0, with very few neurons having significant choice-related activity greater than 0.5 (increasing firing rate for ‘feature-present’ response). Neurons in auditory cortical areas may also modulate their responses to motor events (Brosch 2005). Some previous reports on choice-related activity have been difficult to interpret, as they employed a Go/No-Go task format in which one perceptual choice required a movement and the other choice did not (Brosch 2005; Niwa et al. 2013). Therefore, the choice-related activity observed was difficult to disentangle from a general preparation to move. The task reported here was a Yes/No forced-choice task, requiring a motor response to each decision (target present versus target absent). The shift in choice-related activity between attention conditions observed in this force choice task, and another recent study (Guo et al. 2019) shows that this choice-related activity cannot simply reflect motor preparation or action. This then strengthens the possible relationship between this activity and the decision or attention process.

The lack of clear attentional improvement of single neuron feature encoding found in this study suggests one or more of the following: (1) the feature-selective attention required in this task is not implemented at the level of an individual neuron in A1 or ML; (2) the feature-selective attention necessary for this particular task occurs at a later stage in auditory processing; (3) the mixed selectivity of single neurons in A1 and ML for these features complicates the interpretability of the effects of attention at the single neuron level, in contrast to feature-based attention neurons studied found in visual cortex (Martinez-Trujillo and Treue 2004; Maunsell 2015; Maunsell and Treue 2006). While we did not see robust differences in encoding between attentional conditions, the difference in attentional choice-related activity reveals that it is not simply reflective of motor preparation, and suggests that activity correlated to reported choice as early as A1 could be informing perceptual and decision processes.

References

Angeloni C, **Geffen M**. Contextual modulation of sound processing in the auditory cortex. *Current Opinion in Neurobiology* 49: 8–15, 2018.

Atiani S, **David SV**, **Elgueda D**, **Locastro M**, **Radtke-Schuller S**, **Shamma SA**, **Fritz JB**. Emergent Selectivity for Task-Relevant Stimuli in Higher-Order Auditory Cortex. *Neuron* 82: 486–499, 2014.

Bagur S, **Averseng M**, **Elgueda D**, **David S**, **Fritz J**, **Yin P**, **Shamma S**, **Boubenec Y**, **Ostojic S**. Go/No-Go task engagement enhances population representation of target stimuli in primary auditory cortex. *Nat Commun* 9: 2529, 2018.

Bathellier B, **Ushakova L**, **Rumpel S**. Discrete Neocortical Dynamics Predict Behavioral Categorization of Sounds. *Neuron* 76: 435–449, 2012.

Bizley JK, **Cohen YE**. The what, where and how of auditory-object perception. *Nature Reviews Neuroscience* 14: 693–707, 2013.

Bizley JK, **Walker KMM**, **Nodal FR**, **King AJ**, **Schnupp JWH**. Auditory Cortex Represents Both Pitch Judgments and the Corresponding Acoustic Cues. *Current Biology* 23: 620–625, 2013.

Bregman AS. *Auditory Scene Analysis: The Perceptual Organization of Sc* ess, 1994.

Britten K, **Shadlen M**, **Newsome W**, **Movshon J**. The analysis of visual motion: a comparison of neuronal and psychophysical performance. *The Journal of Neuroscience* 12: 4745–4765, 1992.

Britten KH, **Newsome WT**, **Shadlen MN**, **Celebrini S**, **Movshon JA**. A relationship between behavioral choice and the visual responses of neurons in macaque MT. *Visual Neuroscience* 13: 87–100, 1996.

Brosch M. Nonauditory Events of a Behavioral Procedure Activate Auditory Cortex of Highly Trained Monkeys. *Journal of Neuroscience* 25: 6797–6806, 2005.

Buran BN, **von Trapp G**, **Sanes DH**. Behaviorally Gated Reduction of Spontaneous Discharge Can Improve Detection Thresholds in Auditory Cortex. *Journal of Neuroscience* 34: 4076–4081, 2014.

Carcea I, **Insanally MN**, **Froemke RC**. Dynamics of auditory cortical activity during behavioural engagement and auditory perception. *Nat Commun* 8: 14412, 2017.

Chambers AR, **Hancock KE**, **Sen K**, **Polley DB**. Online Stimulus Optimization Rapidly Reveals Multidimensional Selectivity in Auditory Cortical Neurons. *Journal of Neuroscience* 34: 8963–8975, 2014.

Chen X, **Hoffmann K-P**, **Albright TD**, **Thiele A**. Effect of feature-selective attention on neuronal responses in macaque area MT. *Journal of Neurophysiology* 107: 1530–1543, 2012.

Christison-Lagay KL, **Bennur S**, **Cohen YE**. Contribution of spiking activity in the primary auditory cortex to detection in noise. *Journal of Neurophysiology* 118: 3118–3131, 2017.

Christison-Lagay KL, **Cohen YE**. The Contribution of Primary Auditory Cortex to Auditory Categorization in Behaving Monkeys. *Front Neurosci* 12: 601, 2018.

Downer JD, **Niwa M**, **Sutter ML**. Task Engagement Selectively Modulates Neural Correlations in Primary Auditory Cortex. *Journal of Neuroscience* 35: 7565–7574, 2015.

Downer JD, **Niwa M**, **Sutter ML**. Hierarchical differences in population coding within auditory cortex. *Journal of Neurophysiology* 118: 717–731, 2017a.

Downer JD, **Rapone B**, **Verhein J**, **O'Connor KN**, **Sutter ML**. Feature-Selective Attention Adaptively Shifts Noise Correlations in Primary Auditory Cortex. *The Journal of Neuroscience* 37: 5378–5392, 2017b.

Downer JD, **Verhein JR**, **Rapone BC**, **O'Connor KN**, **Sutter ML**. An emergent population code in primary auditory cortex supports selective attention to spectral and temporal sound features. *bioRxiv* 2020.03.09.984773, 2020.

Elgueda D, **Duque D**, **Radtke-Schuller S**, **Yin P**, **David SV**, **Shamma SA**, **Fritz JB**. State-dependent encoding of sound and behavioral meaning in a tertiary region of the ferret auditory cortex. *Nat Neurosci* 22: 447–459, 2019.

Eliades SJ, **Wang X**. Sensory-Motor Interaction in the Primate Auditory Cortex During Self-Initiated Vocalizations. *Journal of Neurophysiology* 89: 2194–2207, 2003.

Engle JR, **Recanzone GH**. Characterizing spatial tuning functions of neurons in the auditory cortex of young and aged monkeys: a new perspective on old data. *Frontiers in Aging Neuroscience* 4: 36, 2013.

Francis NA, **Elgueda D**, **Englitz B**, **Fritz JB**, **Shamma SA**. Laminar profile of task-related plasticity in ferret primary auditory cortex. *Sci Rep* 8: 16375, 2018a.

Francis NA, **Winkowski DE**, **Sheikhattar A**, **Armengol K**, **Babadi B**, **Kanold PO**. Small Networks Encode Decision-Making in Primary Auditory Cortex. *Neuron* 97: 885-897.e6, 2018b.

Fritz J, **Shamma S**, **Elhilali M**, **Klein D**. Rapid task-related plasticity of spectrotemporal receptive fields in primary auditory cortex. *Nat Neurosci* 6: 1216–1223, 2003.

Fritz JB. Differential Dynamic Plasticity of A1 Receptive Fields during Multiple Spectral Tasks. *Journal of Neuroscience* 25: 7623–7635, 2005.

Fritz JB, **Elhilali M**, **Shamma SA**. Adaptive Changes in Cortical Receptive Fields Induced by Attention to Complex Sounds. *Journal of Neurophysiology* 98: 2337–2346, 2007.

Fusi S, **Miller EK**, **Rigotti M**. Why neurons mix: high dimensionality for higher cognition. *Current Opinion in Neurobiology* 37: 66–74, 2016.

Goldberg JM, **Brown PB**. Response of binaural neurons of dog superior olivary complex to dichotic tonal stimuli: some physiological mechanisms of sound localization. *Journal of Neurophysiology* 32: 613–636, 1969.

Green DM, **Swets JA**. *Signal detection theory and psychophysics*. Huntington, NY: Krieger Publishing Company, 1974.

Grimault N, **Bacon SP**, **Micheyl C**. Auditory stream segregation on the basis of amplitude-modulation rate. *The Journal of the Acoustical Society of America* 111: 1340–1348, 2002.

Gronskaya E, **von der Behrens W**. Evoked Response Strength in Primary Auditory Cortex Predicts Performance in a Spectro-Spatial Discrimination Task in Rats. *J Neurosci* 39: 6108–6121, 2019.

Guo L, **Weems JT**, **Walker WI**, **Levichev A**, **Jaramillo S**. Choice-Selective Neurons in the Auditory Cortex and in Its Striatal Target Encode Reward Expectation. *J Neurosci* 39: 3687–3697, 2019.

Hackett TA. Information flow in the auditory cortical network. *Hearing Research* 271: 133–146, 2011.

Huang Y, **Brosch M**. Associations between sounds and actions in primate prefrontal cortex. *Brain Research* 1738: 146775, 2020.

Huang Y, **Heil P**, **Brosch M**. Associations between sounds and actions in early auditory cortex of nonhuman primates. *eLife* 8: e43281, 2019.

Jaramillo S, **Borges K**, **Zador AM**. Auditory Thalamus and Auditory Cortex Are Equally Modulated by Context during Flexible Categorization of Sounds. *Journal of Neuroscience* 34: 5291–5301, 2014.

Johnson JS, **Niwa M**, **O’Connor KN**, **Sutter ML**. Amplitude modulation encoding in the auditory cortex: comparisons between the primary and middle lateral belt regions. *Journal of Neurophysiology* 124: 1706–1726, 2020.

Kang I, **Maunsell JHR**. Potential confounds in estimating trial-to-trial correlations between neuronal response and behavior using choice probabilities. *Journal of Neurophysiology* 108: 3403–3415, 2012.

Lakatos P, **Musacchia G**, **O’Connel MN**, **Falchier AY**, **Javitt DC**, **Schroeder CE**. The Spectrotemporal Filter Mechanism of Auditory Selective Attention. *Neuron* 77: 750–761, 2013.

Lee C-C, **Middlebrooks JC**. Auditory cortex spatial sensitivity sharpens during task performance. *Nature Neuroscience* 14: 108–114, 2011.

Lemus L, **Hernandez A**, **Romo R**. Neural codes for perceptual discrimination of acoustic flutter in the primate auditory cortex. *Proceedings of the National Academy of Sciences* 106: 9471–9476, 2009.

Lin P-A, **Asinof SK**, **Edwards NJ**, **Isaacson JS**. Arousal regulates frequency tuning in primary auditory cortex. *Proc Natl Acad Sci USA* 116: 25304–25310, 2019.

Mardia KV, **Jupp PE**. *Directional statistics*. Chichester; New York: J. Wiley, 2000.

Martinez-Trujillo JC, **Treue S**. Feature-Based Attention Increases the Selectivity of Population Responses in Primate Visual Cortex. *Current Biology* 14: 744–751, 2004.

Massoudi R, **Van Wanrooij MM**, **Van Wetter SMCI**, **Versnel H**, **Van Opstal AJ**. Task-related preparatory modulations multiply with acoustic processing in monkey auditory cortex. *Eur J Neurosci* 39: 1538–1550, 2014.

Maunsell JHR. Neuronal Mechanisms of Visual Attention. *Annual Review of Vision Science* 1: 373–391, 2015.

Maunsell JHR, **Treue S**. Feature-based attention in visual cortex. *Trends in Neurosciences* 29: 317–322, 2006.

McDermott JH. The cocktail party problem. *Curr Biol* 19: R1024-1027, 2009.

Merzenich MM, **Brugge JF**. Representation of the cochlear partition on the superior temporal plane of the macaque monkey. *Brain Research* 50: 275–296, 1973.

Mirabella G, **Bertini G**, **Samengo I**, **Kilavik BE**, **Frilli D**, **Della Libera C**, **Chelazzi L**. Neurons in Area V4 of the Macaque Translate Attended Visual Features into Behaviorally Relevant Categories. *Neuron* 54: 303–318, 2007.

Ni AM, **Maunsell JHR**. Neuronal Effects of Spatial and Feature Attention Differ Due to Normalization. *J Neurosci* 39: 5493–5505, 2019.

Niwa M, **Johnson JS**, **O'Connor KN**, **Sutter ML**. Active Engagement Improves Primary Auditory Cortical Neurons' Ability to Discriminate Temporal Modulation. *Journal of Neuroscience* 32: 9323–9334, 2012a.

Niwa M, **Johnson JS**, **O'Connor KN**, **Sutter ML**. Activity Related to Perceptual Judgment and Action in Primary Auditory Cortex. *Journal of Neuroscience* 32: 3193–3210, 2012b.

Niwa M, **Johnson JS**, **O'Connor KN**, **Sutter ML**. Differences between Primary Auditory Cortex and Auditory Belt Related to Encoding and Choice for AM Sounds. *Journal of Neuroscience* 33: 8378–8395, 2013.

Niwa M, **O'Connor KN**, **Engall E**, **Johnson JS**, **Sutter ML**. Hierarchical effects of task engagement on amplitude modulation encoding in auditory cortex. *Journal of Neurophysiology* 113: 307–327, 2015.

Nobre AC, **Rao A**, **Chelazzi L**. Selective Attention to Specific Features within Objects: Behavioral and Electrophysiological Evidence. *Journal of Cognitive Neuroscience* 18: 539–561, 2006.

O'Connor KN, **Petkov CI**, **Sutter ML**. Adaptive Stimulus Optimization for Auditory Cortical Neurons. *Journal of Neurophysiology* 94: 4051–4067, 2005.

Osmanski MS, **Wang X**. Behavioral Dependence of Auditory Cortical Responses. *Brain Topogr* 28: 365–378, 2015.

Otazu GH, **Tai L-H**, **Yang Y**, **Zador AM**. Engaging in an auditory task suppresses responses in auditory cortex. *Nature Neuroscience* 12: 646–654, 2009.

Ponvert ND, **Jaramillo S**. Auditory Thalamostriatal and Corticostriatal Pathways Convey Complementary Information about Sound Features. *J Neurosci* 39: 271–280, 2019.

Rauschecker JP, **Tian B**. Mechanisms and streams for processing of "what" and "where" in auditory cortex. *Proceedings of the National Academy of Sciences* 97: 11800–11806, 2000.

Romanski LM, **Tian B**, **Fritz J**, **Mishkin M**, **Goldman-Rakic PS**, **Rauschecker JP**. Dual streams of auditory afferents target multiple domains in the primate prefrontal cortex. *Nature Neuroscience* 2: 1131–1136, 1999.

Ruff DA, **Born RT**. Feature attention for binocular disparity in primate area MT depends on tuning strength. *Journal of Neurophysiology* 113: 1545–1555, 2015.

Runyan CA, **Piasini E**, **Panzeri S**, **Harvey CD**. Distinct timescales of population coding across cortex. *Nature* 548: 92–96, 2017.

Saleem K, **Logothetis Nikos K**. *A combined MRI and histology atlas of the rhesus monkey brain in sterotaxic coordinates*. Burlington, MA: Academic Press, 2007.

Sasaki R, **Uka T**. Dynamic Readout of Behaviorally Relevant Signals from Area MT during Task Switching. *Neuron* 62: 147–157, 2009.

Schneider DM, **Nelson A**, **Mooney R**. A synaptic and circuit basis for corollary discharge in the auditory cortex. *Nature* 513: 189–194, 2014.

Schnupp JWH. Plasticity of Temporal Pattern Codes for Vocalization Stimuli in Primary Auditory Cortex. *Journal of Neuroscience* 26: 4785–4795, 2006.

Schwartz ZP, **Buran BN**, **David SV**. Pupil-associated states modulate excitability but not stimulus selectivity in primary auditory cortex. *Journal of Neurophysiology* 191–208, 2019.

Schwartz ZP, **David SV**. Focal Suppression of Distractor Sounds by Selective Attention in Auditory Cortex. *Cerebral Cortex* 28: 323–339, 2018.

Scott BH, **Malone BJ**, **Semple MN**. Effect of Behavioral Context on Representation of a Spatial Cue in Core Auditory Cortex of Awake Macaques. *Journal of Neuroscience* 27: 6489–6499, 2007.

Shannon RV, **Zeng F-G**, **Kamath V**, **Wygonski J**, **Ekelid M**. Speech Recognition with Primarily Temporal Cues. *Science* 270: 303–304, 1995.

Shinn-Cunningham BG. Object-based auditory and visual attention. *Trends in Cognitive Sciences* 12: 182–186, 2008.

Strickland EA, **Viemeister NF**. The effects of frequency region and bandwidth on the temporal modulation transfer function. *The Journal of the Acoustical Society of America* 102: 1799–1810, 1997.

Sutter ML, **Shamma SA**. The Relationship of Auditory Cortical Activity to Perception and Behavior. In: *The Auditory Cortex*, edited by Winer JA, Schreiner CE. Springer US, p. 617–641.

Tian B, **Rauschecker JP**. Processing of Frequency-Modulated Sounds in the Lateral Auditory Belt Cortex of the Rhesus Monkey. *Journal of Neurophysiology* 92: 2993–3013, 2004.

von Trapp G, **Buran BN**, **Sen K**, **Semple MN**, **Sanes DH**. A Decline in Response Variability Improves Neural Signal Detection during Auditory Task Performance. *Journal of Neuroscience* 36: 11097–11106, 2016.

Treue S, **Trujillo JCM**. Feature-based attention influences motion processing gain in macaque visual cortex. *Nature* 399: 575–579, 1999.

Tsunada J, **Lee JH**, **Cohen YE**. Representation of speech categories in the primate auditory cortex. *Journal of Neurophysiology* 105: 2634–2646, 2011.

Tsunada J, **Liu ASK**, **Gold JI**, **Cohen YE**. Causal contribution of primate auditory cortex to auditory perceptual decision-making. *Nature Neuroscience* 19: 135–142, 2016.

Uka T, **Sasaki R**, **Kumano H**. Change in Choice-Related Response Modulation in Area MT during Learning of a Depth-Discrimination Task is Consistent with Task Learning. *Journal of Neuroscience* 32: 13689–13700, 2012.

Van Tasell DJ, **Soli SD**, **Kirby VM**, **Widin GP**. Speech waveform envelope cues for consonant recognition. *The Journal of the Acoustical Society of America* 82: 1152–1161, 1987.

Wang L, **Narayan R**, **Grana G**, **Shamir M**, **Sen K**. Cortical Discrimination of Complex Natural Stimuli: Can Single Neurons Match Behavior? *Journal of Neuroscience* 27: 582–589, 2007.

Woods KJP, **McDermott JH**. Attentive Tracking of Sound Sources. *Current Biology* 25: 2238–2246, 2015.

Yin P, **Fritz JB**, **Shamma SA**. Rapid Spectrotemporal Plasticity in Primary Auditory Cortex during Behavior. *Journal of Neuroscience* 34: 4396–4408, 2014.

Yin P, **Johnson JS**, **O'Connor KN**, **Sutter ML**. Coding of Amplitude Modulation in Primary Auditory Cortex. *Journal of Neurophysiology* 105: 582–600, 2011.

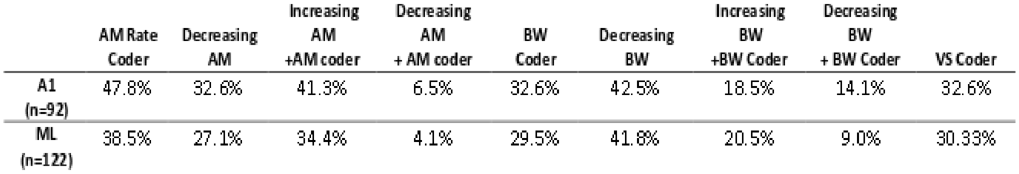

	AM Rate Coder	Decreasing AM	Increasing AM +AM coder	Decreasing AM + AM coder	BW Coder	Decreasing BW	Increasing BW +BW Coder	Decreasing BW + BW Coder	VS Coder
A1 (n=92)	47.8%	32.6%	41.3%	6.5%	32.6%	42.5%	18.5%	14.1%	32.6%
ML (n=122)	38.5%	27.1%	34.4%	4.1%	29.5%	41.8%	20.5%	9.0%	30.33%

Table 1.1: Percentage of cells in A1 and ML that increased firing rate in response to each feature dimension vs. those that decreased activity in response to the feature dimension. The majority of cells that significantly encoded AM (AM coder) in both A1 and ML increased firing rate in the presence of AM sounds. Cells that significantly encoded ∆BW (BW Coder) in A1 were about equally likely to be increasing as decreasing. BW coders in ML were more likely to have increasing functions than decreasing.

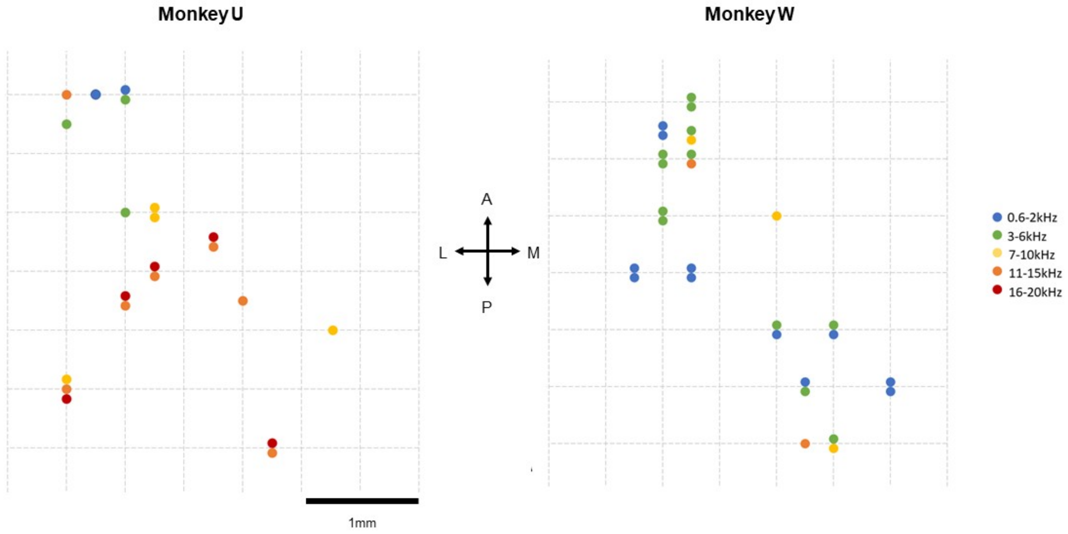

Figure 1.1. Tonotopic maps for both animals. We have included here tuning preferences from sessions that were not included in this study to present a fuller example of the recording areas. These maps represent the recording chambers and positions within them.

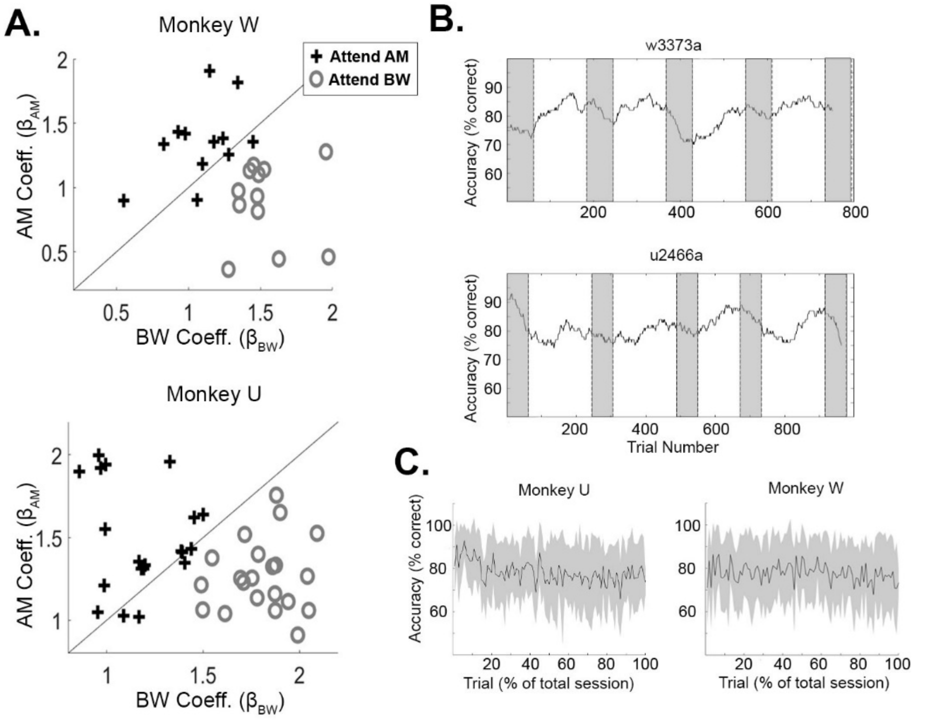

Figure 1.2. Animals' behavioral performance. **A**. Performance of each animal by attention condition, shown by the regression coefficients that correspond to the influence of each feature on the animals' response. Each symbol identifies a single recording session. Increases in coefficient values represent an increased probability that the animal will report 'yes' as the level of that feature increases. Both animals' behavioral responses are influenced more strongly by the target feature than the distractor feature. This is analysis is identical to that of Downer et al. 2017b, but now has added the ML sessions. **B.** Examples of performance over time during a behavioral session. Performance would fluctuate across a session, but did not tend to systematically get worse near the end of the session. Grey rectangles indicate instruction trials at the beginning of a new block. **C.** Average performance across all sessions by percent of total trials for each monkey.

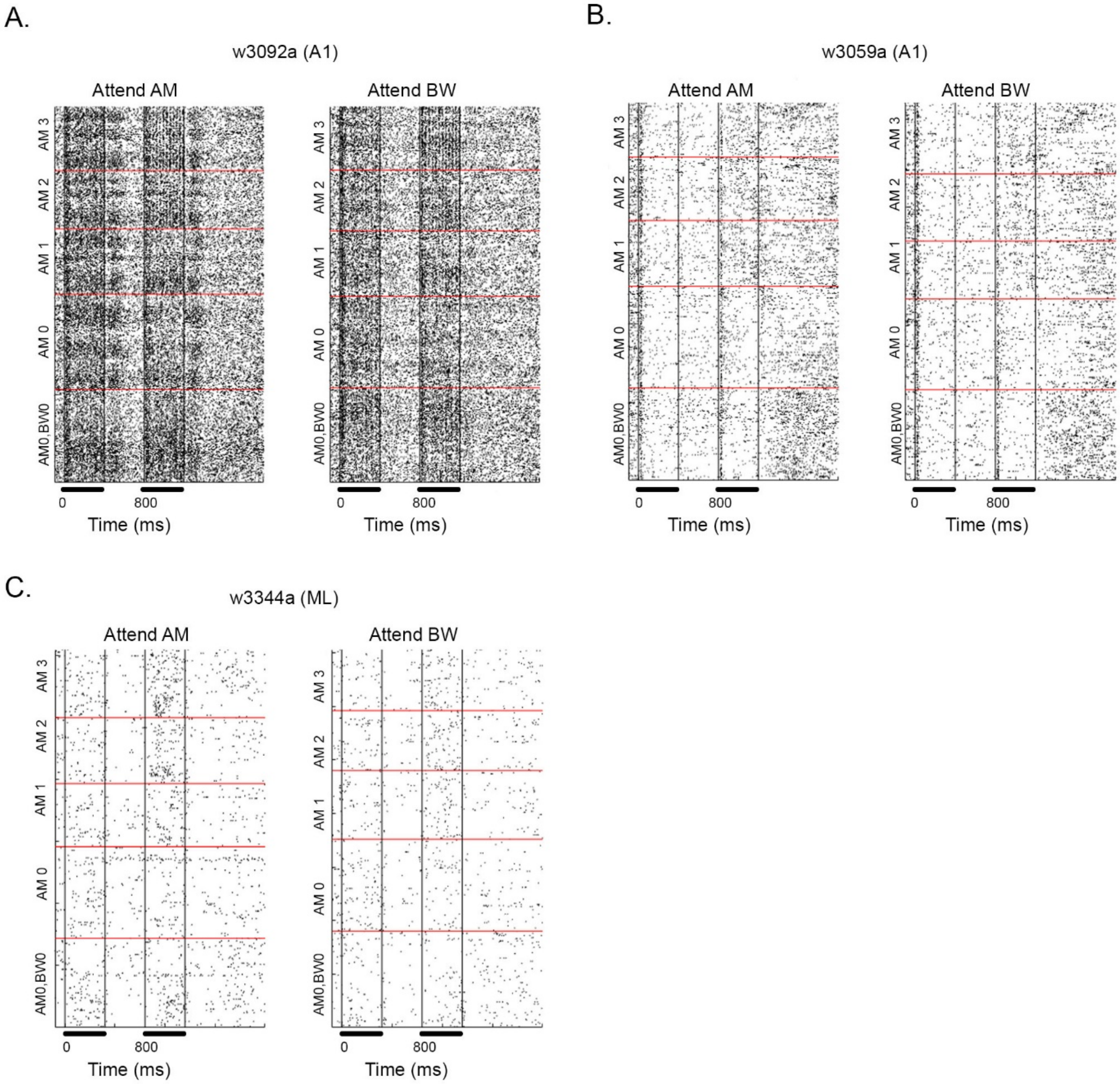

Figure 1.3. Example responses of A1 (A, B) and ML (C) neurons to AM noise by attentional condition. On the largest scale we sort by S2 stimulus. The lowest rectangle in each had no AM and no bandwidth restriction (AM0, BW0). Then the going up the next rectangle (AM0) shows the responses to stimuli with no AM but with BW restriction (within the rectangle sorted from lowest on bottom to highest level of BW restriction). The three different levels of stimuli with AM and BW restriction are then shown above. For these within each rectangle the sorting by BW restriction is the same as for AM0. Each sub-plot is separated into “Attend AM” trials (left) and “Attend BW” trials (right). Bars below each plot indicate stimulus presentation. Black bars below time axis indicate presentation of the S1 and S2 stimulus. **A)** This neuron encoded AM with average firing rate and vector strength (VSpp), and encoded BW with firing rate. (Definitions of ‘encoding’ are statistically-based and in the methods). **B)** Encoded AM with firing rate but not with VSpp and did not encode BW. **C)** Encoded AM and BW with firing rate, but did not use VSpp to encode AM.

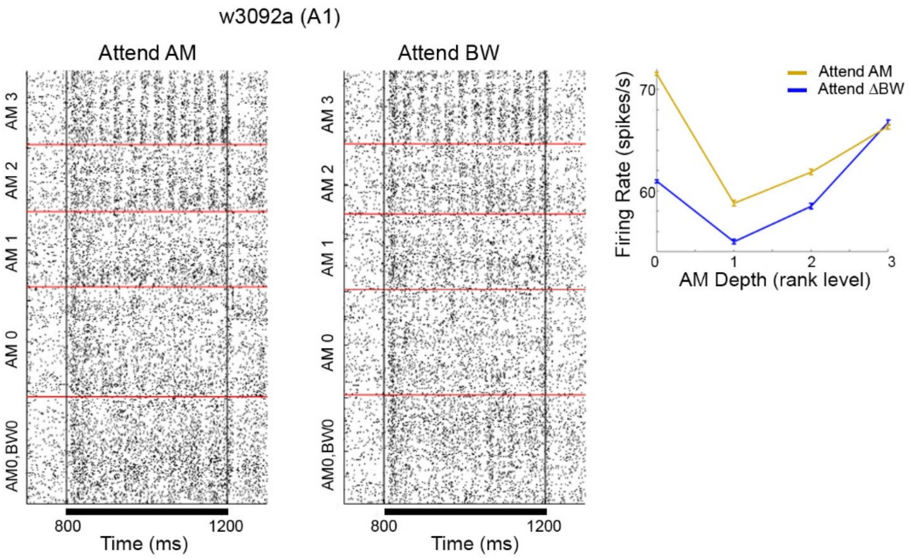

Figure 1.4. Same example cell from Figure 1.3a, with the peri-S2 time window expanded. Inset shows firing rate as a function of AM depth, error bars show SE. The unmodulated stimuli (AM0) had significantly higher firing rates in the attend AM versus the attend BW condition. While the firing rate appears higher in the other AM stimuli (AM1,2,3) during attend-AM, none of those AM stimuli showed significant changes in activity between attend-AM and attend BW

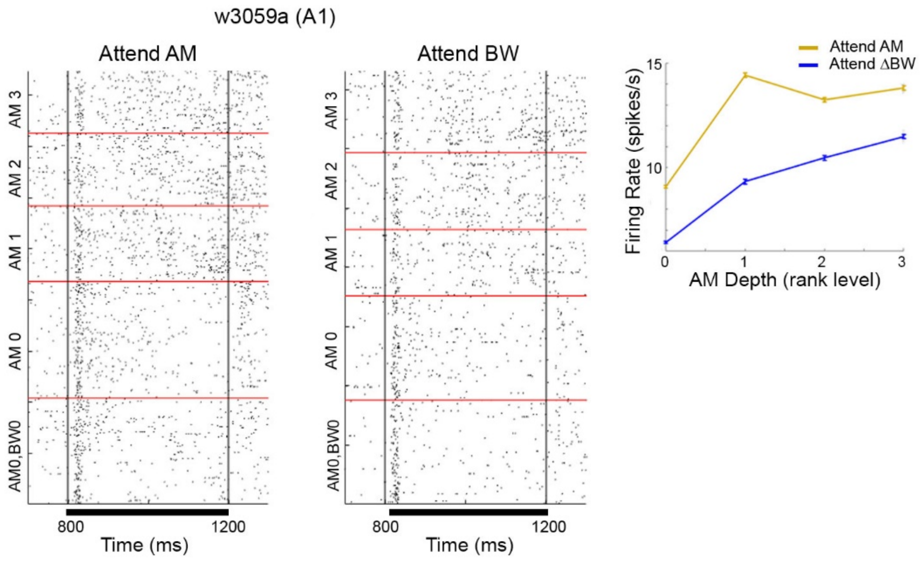

Figure 1.5. Same as example cells as in Figure 1.3b, with the peri-S2 time window expanded. Inset shows firing rate as a function of AM depth, error bars show SE. Firing rate in response to AM0 and AM1 was significantly greater in attend AM than Attend BW.

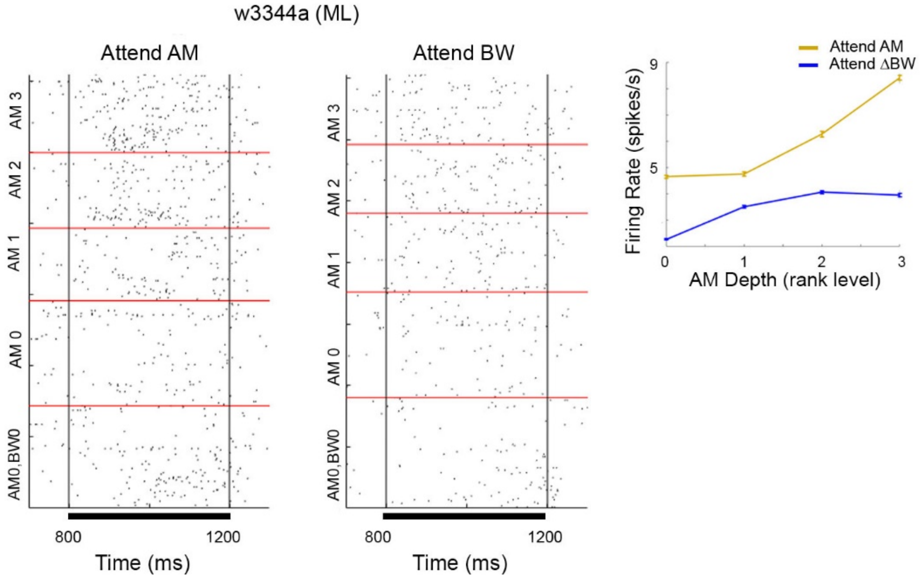

Figure 1.6. Same example cell as in Figure 1.3c, with the peri-S2 time window expanded. Inset shows firing rate as a function of AM depth, error bars show SE. For all conditions firing rate was higher in attend AM, but this was only significant for unmodulated (AM0) and the most modulated (AM3).

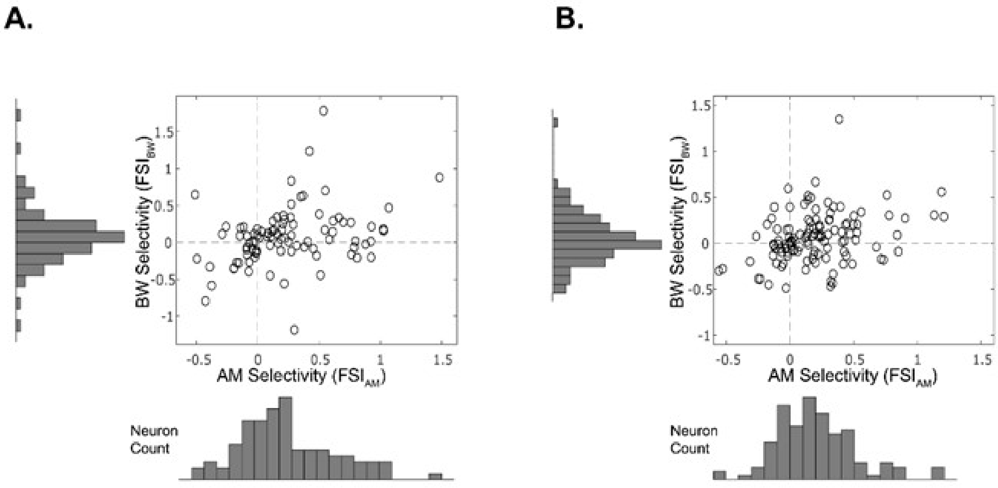

Figure 1.7: Single neuron feature selectivity index (FSI), a measure of how sensitive a neuron is to changes in each feature value separately. **A.** A1: a positive correlation between AM and ∆BW selectivity (Pearson rho = 0.3143, *p* = 0.002) **B.** ML: positive correlation between AM and BW selectivity (Pearson's rho = 0.3109, *p* = 5.32 e-4)

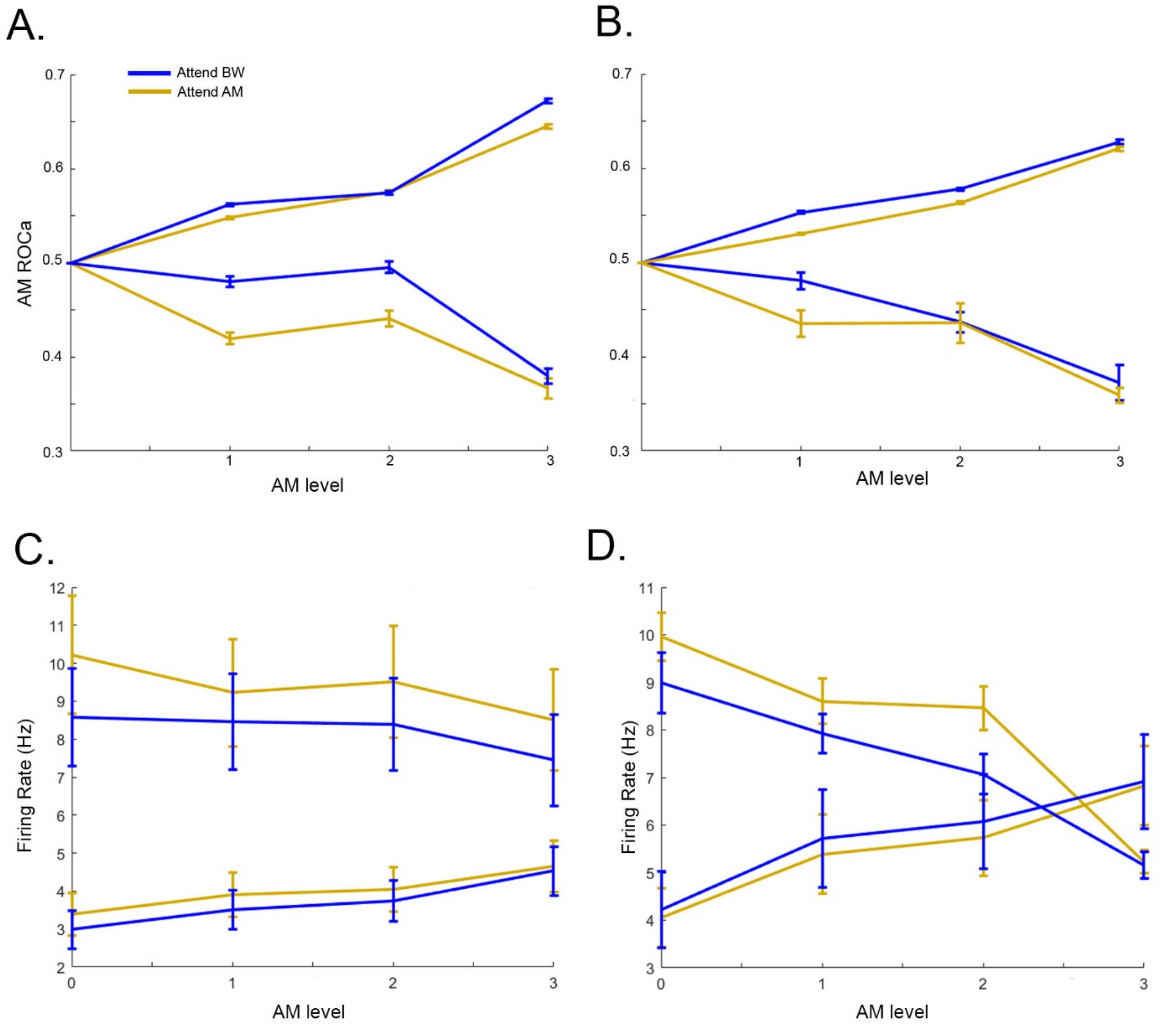

Figure 1.8. Population average rate-based responses to AM level in A1 (AC) and ML (BD). As AM depth increased, AM discrimination tended to get better (ROCa further away from 0.5). Blue lines indicate responses during Attend BW context, yellow lines indicate responses during Attend AM condition. **A)** AM encoding (ROCa) in A1. Here we include only cells that were *significant AM encoders* (n=38 increasing, n=6 decreasing cells)**. B)** AM encoding (ROCa) in ML. Here we include only cells that were *significant AM encoders* (n=42 increasing, n=5 decreasing cells). **CD)** Population average raw firing rate for *all* A1 (**C**, n = 92) and ML (**D**, n = 122). Each plot is separated by 'increasing cells' (A1 n = 62, ML n = 89) and 'decreasing cells' (A1 n = 30, ML n = 33).

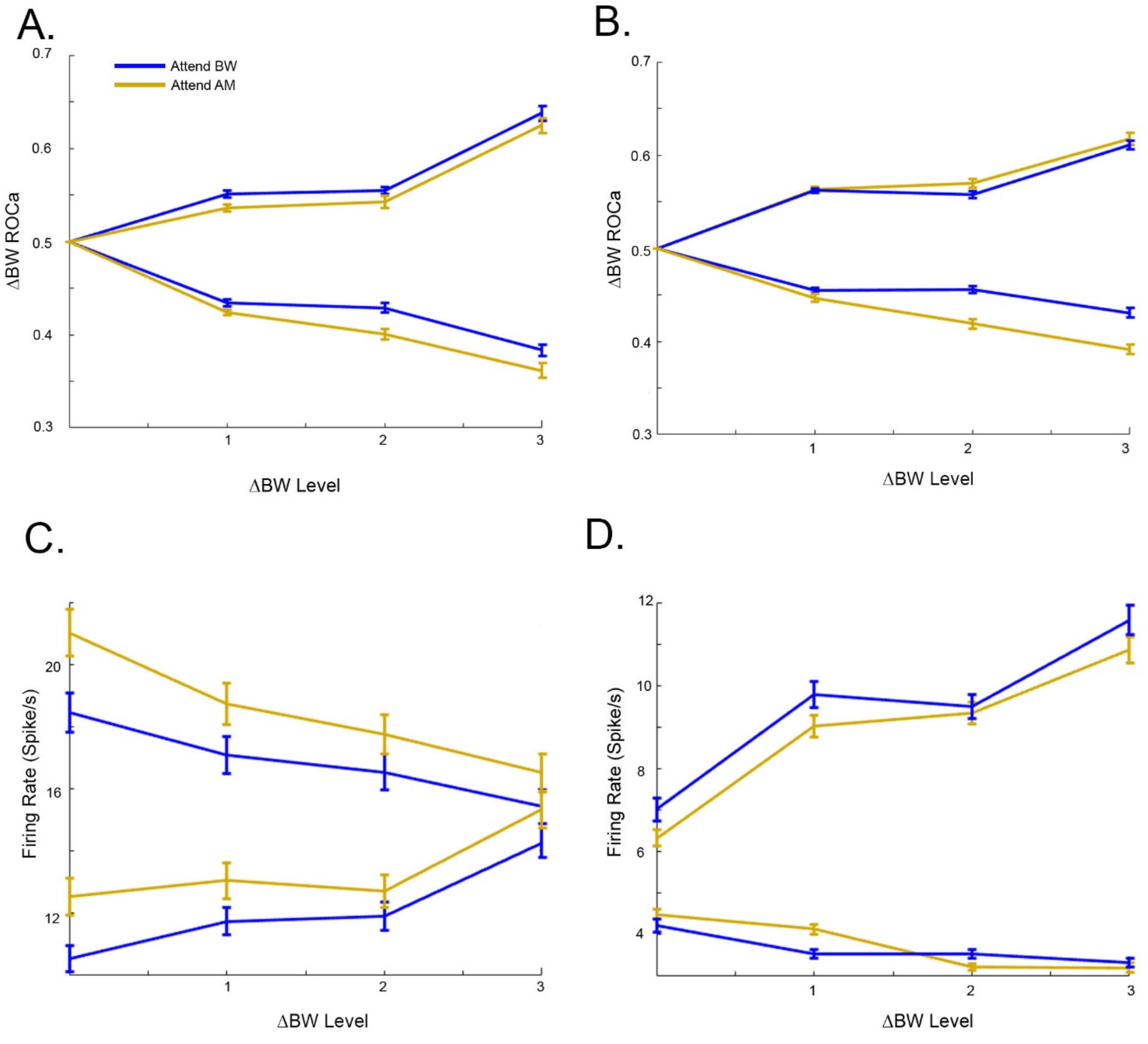

Figure 1.9. As in 1.6, for the BW feature dimension. Population averaged responses to BW level. As ΔBW increased, BW encoding tended to get better (ROCa further away from 0.5) Blue lines indicate attend BW condition, yellow lines indicate attend AM condition. **A)** BW encoding (ROCa) in A1. Here we include *only cells that significantly encoded ΔBW* (n = 17 increasing, n = 13 decreasing cells). **B)** BW encoding (ROCa) in ML. Here we include *only cells that were significant BW encoders* (n = 25 increasing, n = 11 decreasing cells). **CD)** Population average raw firing rate by ΔBW level for *all* A1 (**C**, n = 92) and ML (**D**, n = 122). Each plot is separated by 'increasing cells' (A1 n = 53, ML n = 86) and 'decreasing cells' (A1 n = 39, ML n = 36). There was no significant effect of attentional condition at any level of ΔBW for either A1 (**AC**) or ML (**BD**).

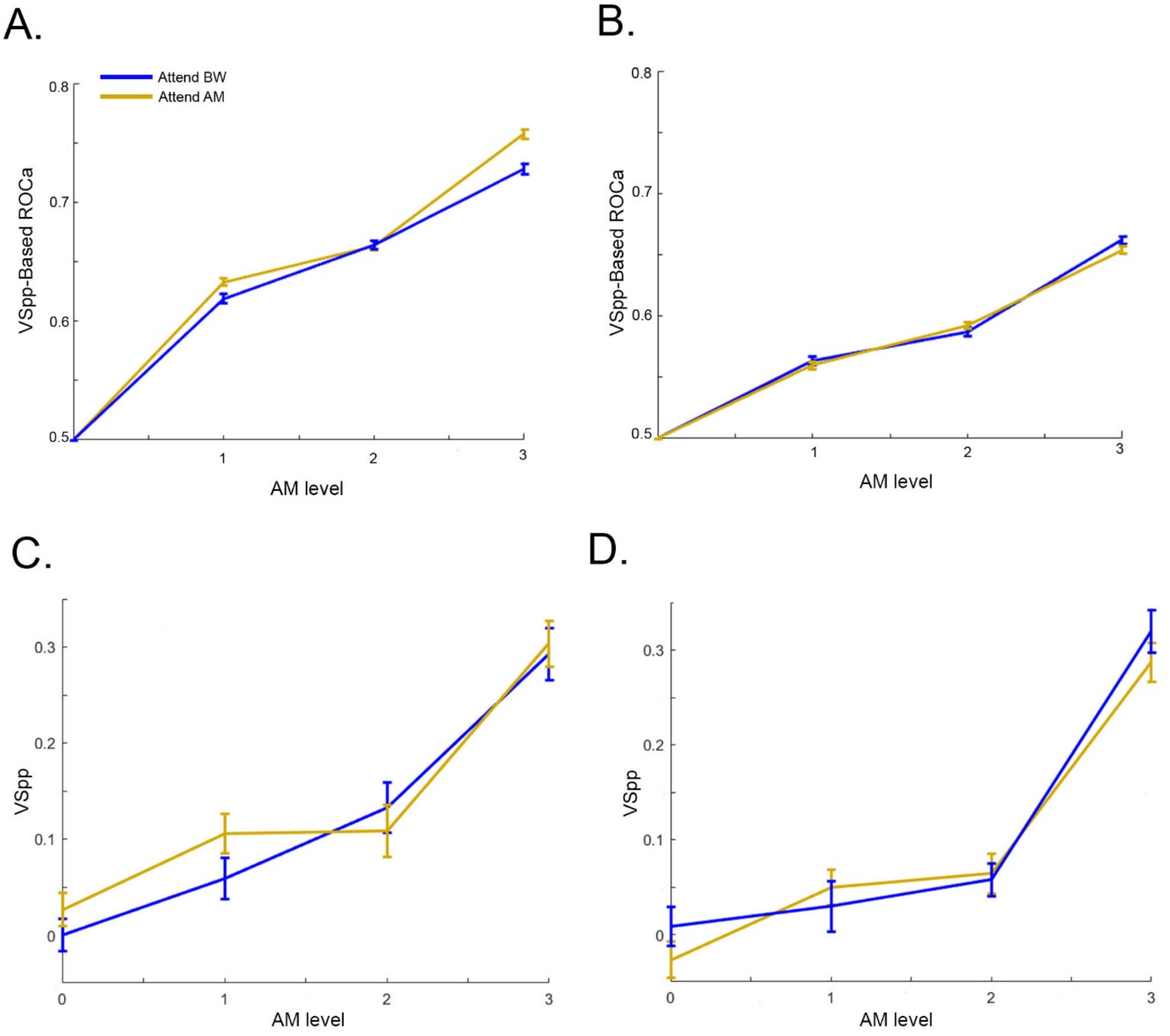

Figure 1.10. Population averaged phase locking responses to AM. Yellow lines indicate attend AM condition, blue lines indicate attend BW condition. **AB)** VS_{pp}-based discriminability (ROCa) of AM from unmodulated sounds. In both A1(**A**, n = 30) and ML (**B**, n = 37), VS_{pp}-based discriminability of AM was not significantly different between attention conditions at any AM level ($p > 0.05$, signed-rank test) At low modulation depths (AM level = 1), A1 had significantly better AM discriminability than ML ($p = 0.02$, Wilcoxon rank sum test), however they were not significantly different at the higher modulation depths (AM levels 2 and 3, $p > 0.05$, Wilcoxon rank sum test). **CD)** Population averaged phase locking responses (VSpp) in *all cells* for A1 (**C,** n=92) and ML (**D**, n = 122). VSpp is greater in A1 **(C)** than ML **(D)** at low AM depths (AM level 1, $p = 0.01$; AM level 2, $p = 0.002$, Wilcoxon ranked sum test), though phase locking is more similar (not significantly different) at the highest AM depth ($p = 0.73$, Wilcoxon ranked sum). There was no significant difference in either VSpp between attentional conditions in either area ($p > 0.05$ for all AM levels, Wilcoxon signed rank test).

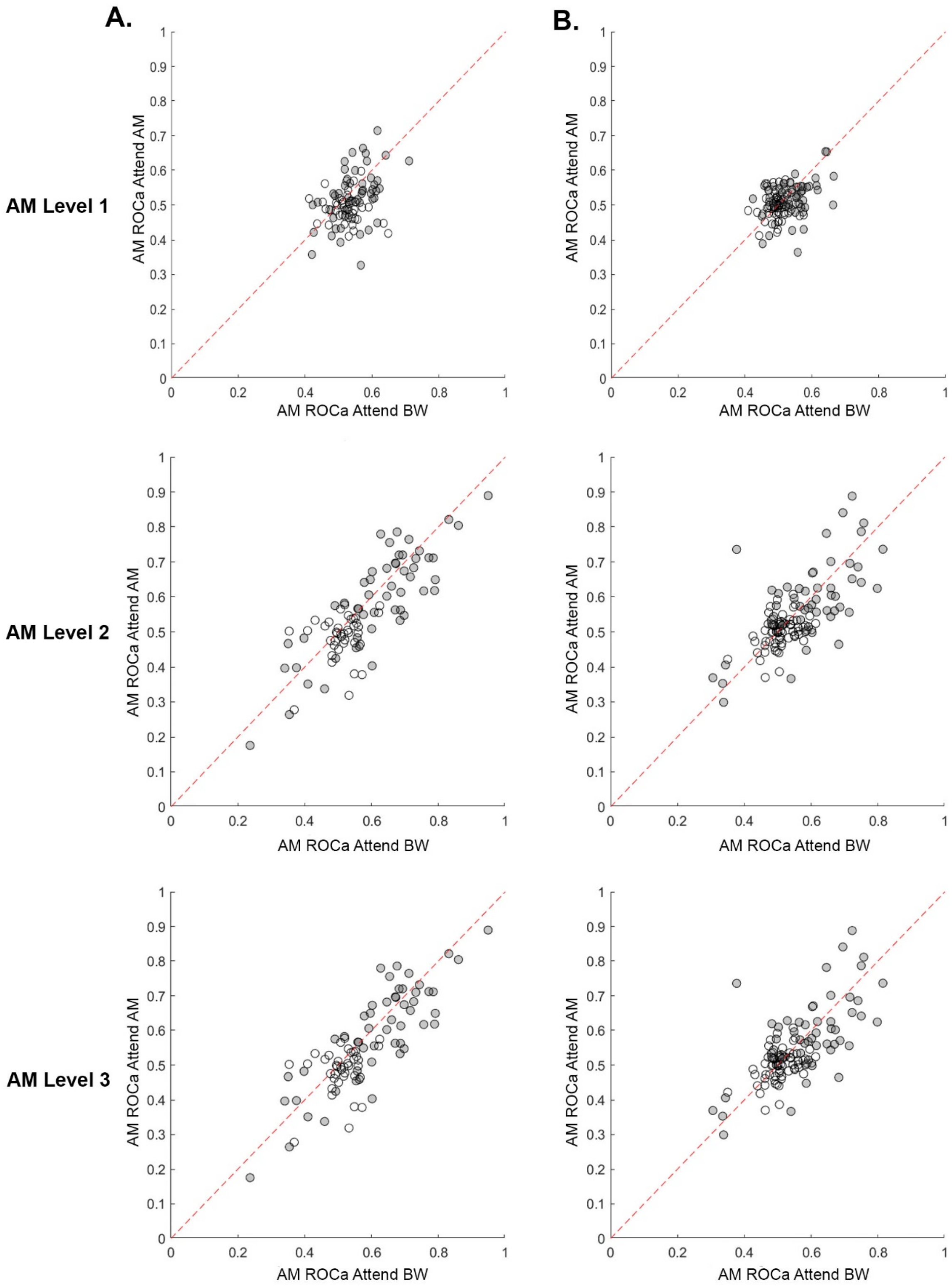

Figure 1.11. Cell-by-cell AM firing rate encoding differences between attention conditions for **A.** A1 (n=92) and **B.** ML (n = 122) Filled dots indicate cells that significantly encode AM. Diagonal line is the unity line. As feature level increased, discriminability of AM from unmodulated sounds became greater (ROCa further away from 0.5).

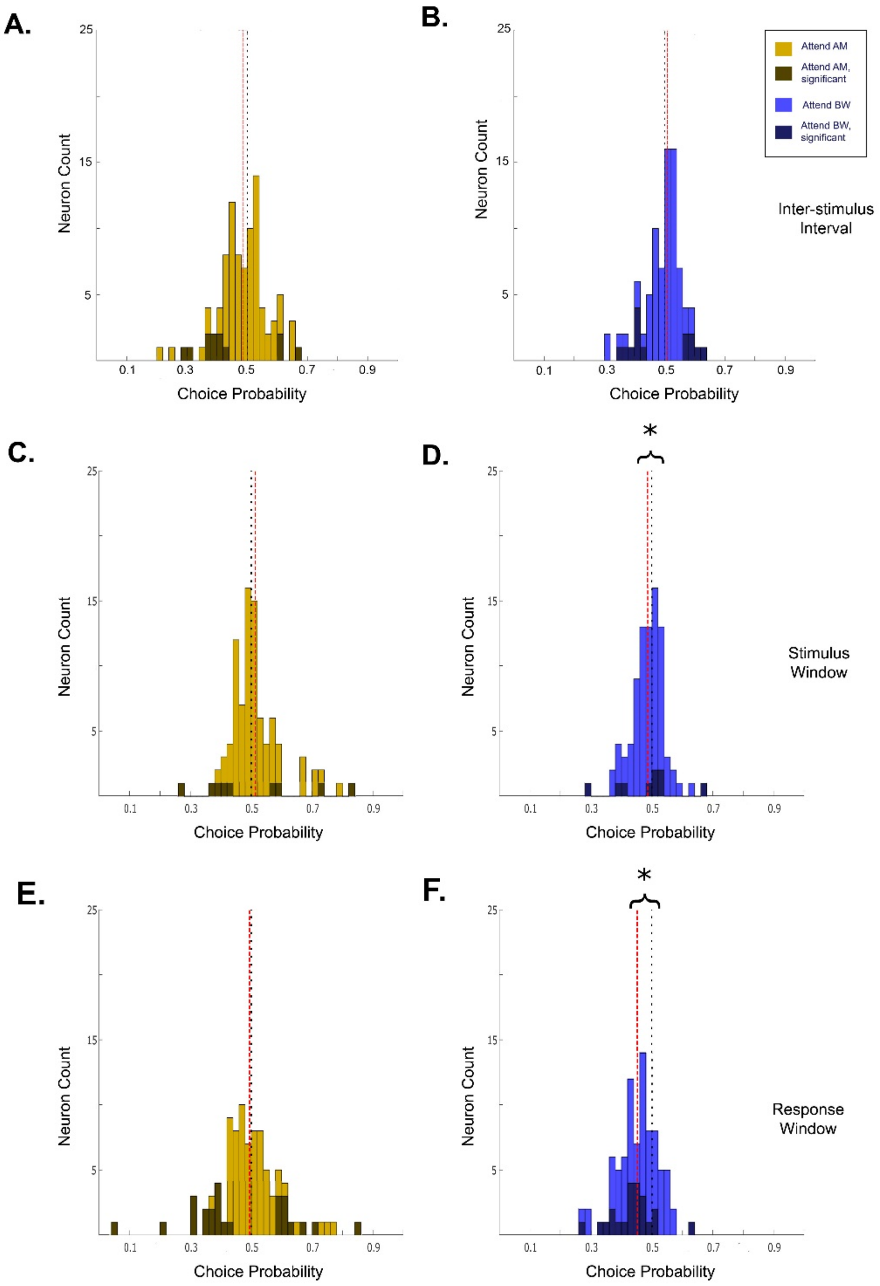

Figure 1.12: Choice probability in A1 (n = 92). Values closer to 0 indicate increased activity for 'feature-absent' response, whereas 1 indicates increased activity for 'feature-present' response. Darker colored bars indicate cells with significant choice activity. Black dotted line indicates 0.5, red dashed line denotes the population median. **A, B.** CP during the ISI window was centered about 0.5 for both **A.** the attend AM condition (median = 0.49, p = 0.11, signed-rank test) and **B.** the attend BW condition (median = 0.51, p = 0.92, signed-rank test). CP during the attend AM condition is evenly distributed about 0.5 in both **C.** the stimulus window (median = 0.50, p = 0.87, signed-rank test) and **E.** the response window (median = 0.49, p = 0.43, signed-rank test). In the attend ΔBW condition, CP values tended to be less than 0.5 in both **D.** the stimulus window (median = 0.49, p = 0.02 signed-rank test) and **F.** the response window (median = 0.46, p = 4.2 e-8 signed-rank test). There was a significant difference in the population CP distributions between attention conditions during the RW (p = 0.004, signed-rank test), though not during the S2 (p = 0.06, signed-rank test).

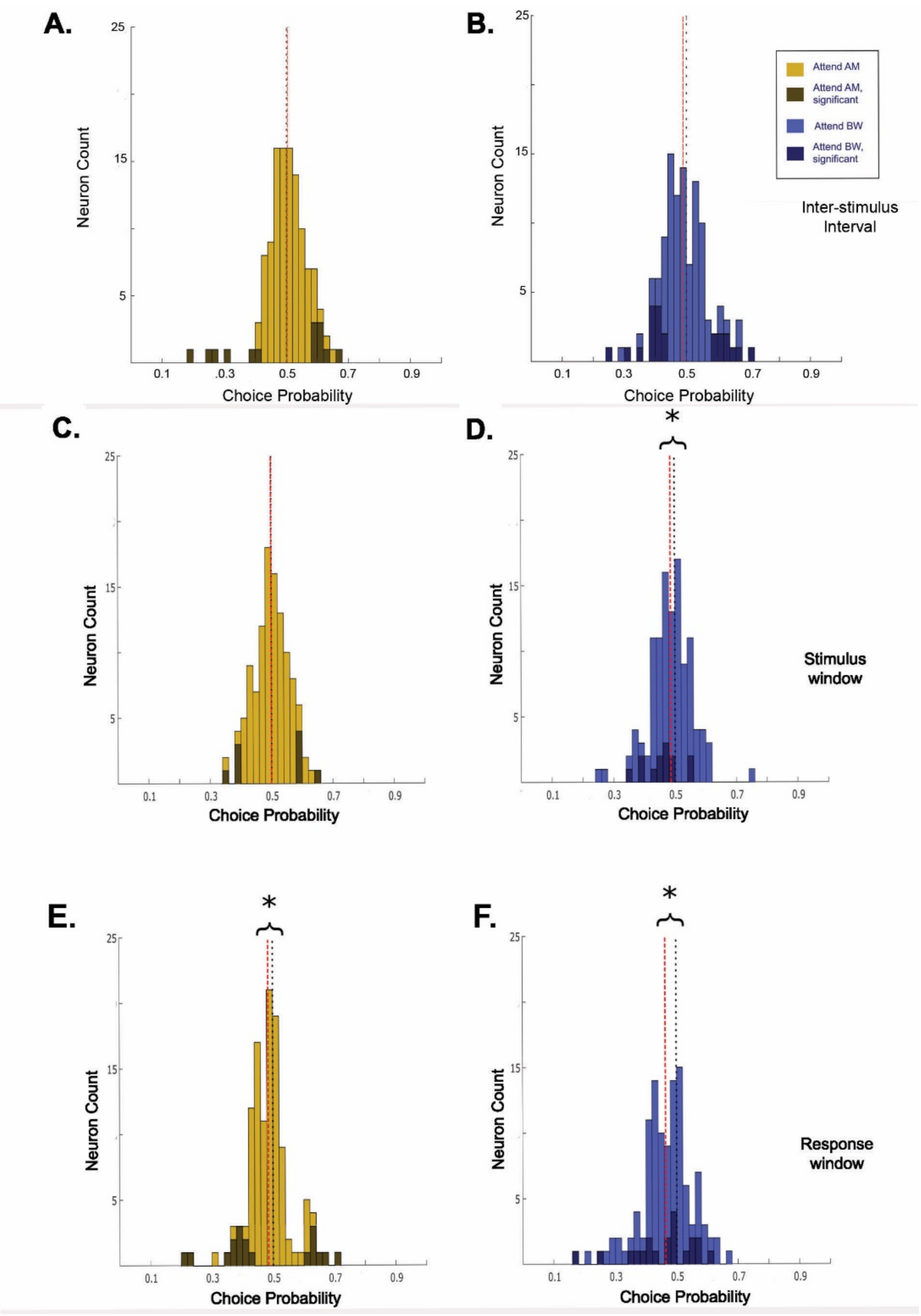

Figure 1.13: Choice probability in ML (n = 122), as in Figure 1.5. **A, B.** CP during the ISI window was centered about 0.5 for both **A.** the attend AM condition (median = 0.50, *p* = 0.47, signed-rank test) and **B.** the attend BW condition (median = 0.49, *p* = 0.15, signed-rank test). CP during the attend AM condition is evenly distributed about 0.5 in **C.** the stimulus window (median = 0.50, *p* = 0.94, signed-rank test). However, in the response window **E.** CP values tended to be less than 0.5 (median = 0.48, *p* = 0.004, signed-rank test). In the attend ∆BW condition, CP values tended to be less than 0.5 in both **D.** the stimulus window (median = 0.49, *p* = 0.043 signed-rank test) and **F.** the response window (median = 0.47, *p* = 2.7 e-5 signed-rank test). As in A1, there was a significant difference in the population CP distributions between attention conditions during the RW (*p* = 0.033, signed-rank test), though not during the S2 (*p* = 0.15, signed-rank test).

Chapter 2

Effects of attention on auditory sensory encoding and choice-related activity in during a novel intermodal attention task

Abstract

Attention studies in auditory cortex have largely been comprised of experiments in which comparisons are made between passive presentation of sounds and a condition in which animals are performing some sort of auditory task. This leads to ambiguity as to whether differences in neural activity between conditions are an effect of selective attention or a more general mechanism such as arousal. To disentangle these effects, we recorded single units in primary and secondary auditory cortex of two Rhesus macaques trained on an audiovisual intermodal attention task. Subjects switched between blocks of performing an auditory discrimination task, while ignoring visual stimuli and blocks of performing a visual discrimination task while ignoring the auditory stimuli. Unimodal instruction blocks were presented prior to each bimodal block to cue the subject to the upcoming target modality. We found that neural discriminability of the auditory stimulus was significantly better during the unimodal auditory presentation than either of the bimodal conditions, however we found few differences in discriminability between the attend auditory bimodal and the attend visual bimodal condition. This suggests that while the presence of a distracting modality has a large effect on neural discriminability, attending to the auditory stimulus, compared with actively ignoring it does not greatly impact single-unit neural discriminability.

Introduction

One of the questions that remains at the forefront of neuroscience is: what precisely is attention and what are the neural mechanisms that underlie it? Attention is a critical behavior that allows us to sift through the vast amount of perceptual information in the environment to focus on that most relevant to current behavioral goals while ignoring distracting information. This has most commonly been studied in auditory cortex using an active engagement approach: where neural responses to sounds are compared when a subject is engaging with the stimuli versus when the subject passively listens to the same stimuli. While this approach has led to many interesting insights into how engaging with a sound can change neural responses (Bagur et al. 2018; Downer et al. 2015; Fritz et al. 2007; Niwa et al. 2012a, 2015; Otazu et al. 2009), it leaves open the question as to whether these changes are due to selective attention mechanisms or attributed to more general changes in arousal states.

Studies investigating selective attention at the physiological level are rare in auditory cortex (Downer et al. 2017; O’Connell et al. 2014; Schwartz and David 2018), though are more common in the visual system (Cohen and Maunsell 2011; Desimone and Duncan 1995; Mirabella et al. 2007; Ni and Maunsell 2019; Rodgers and DeWeese 2014; Wimmer et al. 2015). As reviewed by (Maunsell 2015), selective attention has been shown to change response magnitude, latency, variability, as well as interneuronal correlations in the visual system. Additionally, these changes tend to be greater at later stages in the visual hierarchy (Maunsell and Cook 2002). However, it is unclear if these mechanisms are similar in the auditory system.

Intermodal attention, where the competing stimuli are from different modalities, has not been well studied in single-unit physiology (Hocherman et al. 1976; Mehta 2000a, 2000b; O’Connell et al. 2014). Yet, this is a common situation in our daily lives; for example, reading a book while music plays. If a particularly catchy song comes on, it’s likely that one would be distracted from their reading and listen before returning to their reading. This type of attention has been studied more at the cognitive neuroscience level, where it has been shown that attending to auditory stimuli over other modalities can increase sustained auditory responses (Saupe 2009; Saupe et al. 2009), increase frequency following responses in auditory cortex (Hartmann and Weisz 2019), and effect early stages of sensory encoding

(Karns and Knight 2009) compared to when the auditory stimuli are being ignored (Hartmann and Weisz 2019; Karns and Knight 2009; Saupe 2009; Saupe et al. 2009). Studies that have investigated this at the single neuron level have shown increased response strength to stimuli when they were attended (Hocherman et al. 1976; Mehta 2000a, 2000b), however, it is unclear how these attentional changes may affect the task-relevant encoding of more complex stimuli.

In addition to sensory related activity, auditory cortex has been reported to have activity related to other behaviorally relevant information, including visual and somatosensory stimuli (Bizley and King 2009; Brosch 2005; Kayser et al. 2005, 2008; Lemus et al. 2010; Maddox et al. 2015), choice-related activity (Bizley et al. 2013; Guo et al. 2019; Niwa et al. 2012b, 2013; Tsunada et al. 2016), and reward expectation (Brosch et al. 2011; David et al. 2012; Guo et al. 2019). It remains unclear whether choice-related activity in auditory cortex reflects feedforward processes of sensory information providing evidence for perceptual decisions, or whether it originates from feedback processes from higher areas related to decision making or motor planning (Francis et al. 2018; Niwa et al. 2013; Stoilova et al. 2020; Tsunada et al. 2016) In this study, we utilize trials in which animals are performing perceptual decisions on unimodal visual stimuli to disentangle feedforward compared with feedback related origins of choice-related activity in auditory cortical neurons. In a feedforward model, we would expect choice-related activity to be largely extinguished in auditory cortex during unimodal visual trials, whereas it is possible that if this activity is reflective of feedback choice-related activity may persist during unimodal visual trials.

Here, we designed and trained Rhesus macaques on a difficult intermodal attention task. Stimuli in both the auditory and visual modalities spanned the subjects' perceptual range from sub-threshold of detection to far supra-threshold. We recorded from neurons in primary auditory cortex (A1) and middle lateral belt (ML) while animals were presented with bimodal stimuli and switched between performing an auditory task and performing a visual task. Subjects were cued as to which modality should be attended with a unimodal instruction block preceding each bimodal block. We found both rate and temporal encoding of amplitude modulated noise was better in the unimodal auditory block than either of the bimodal blocks. However, there were few differences between the two bimodal attentional contexts. We also found a large population of cells in both A1 and ML with overall firing rates that were modulated by attentional context, regardless of how well they encoded the relevant auditory stimulus features.

Materials and Methods

Subjects

Subjects were two adult rhesus macaques, one male (13kg, 19 years old), one female (9kg, 12 years old). All procedures were approved by the University of California Davis Animal Care and Use Committee and met the requirements of the United States Public Health Service policy on experimental animal care.

Recording Procedures

Each animal was implanted using aseptic surgical techniques with a headpost centrally behind the brow ridge and a recording chamber over and 18mm craniotomy above the left parietal lobe. Craniotomy placement was based on stereotactic coordinates of auditory cortex to allow for vertical access through parietal cortex to the superior temporal plane (Saleem and Logothetis 2007).

Recordings took place in a sound attenuating, foam lined booth (IAC: 2.9 x 3.2 x 2 meters) while subjects sat in an acoustically transparent primate chair (Crist Instruments). One to three quartz coated tungsten microelectrodes (Thomas Recording, 1-2 MΩ, 0.35mm horizontal spacing) were advanced vertically to auditory cortex. Extracellular signals were amplified (AM Systems model 1800), bandpass filtered between 0.3Hz – 10kHz (Krohn-Hite 3382), and converted into a digital signal at a 50kHz sampling rate (CED model 1401). As electrodes were advanced, a variety of sounds were presented to identify auditory responsive neurons. Subjects sat passively while auditory responsive neurons were isolated. Once at least one auditory responsive single unit was identified, pure tone tuning responses as well as bandpass noise responses were recorded for identification of cortical area. Once tuning properties were recorded, the behavioral session began.

Identification of Cortical Field

Recording locations were identified using stereotactic coordinates (Martin and Bowden 1996) as well as established physiological measures (Merzenich and Brugge 1973; Rauschecker and Tian 2004; Tian and Rauschecker 2004). Boundaries of A1 and ML were assessed with tonotopic gradient reversal, BW responses, spike latency, response robustness to pure tones, and grid location. Recording sessions were assigned to putative cortical fields *post hoc* using these metrics.

Behavioral Paradigm

Animals were presented with audio-visual stimuli and alternated blocks of performing an auditory task with blocks of performing a visual task. Animals were trained on each modality separately and behavioral discrimination thresholds were determined unimodally before being presented bimodal stimuli. Both tasks were two-alternative forced choice where the subject responded using a joystick motion either up or down.

Auditory Task

Subjects were presented with broadband noise that had been sinusoidally amplitude modulated (AM) and performed an AM frequency discrimination task. Each trial consisted of two, 400ms sounds separated by a 400ms interstimulus interval (ISI). The first stimulus (S1) was AM noise at 100% modulation depth; the second stimulus (S2) was AM noise that was 0.717 octaves either higher or lower in frequency than the S1. Subjects reported whether the S2 was higher or lower in AM frequency than the S1, all correct responses were rewarded with a small drop of juice and all incorrect responses were rewarded with a brief (3-4s) timeout (Figure 2.1). The S2 was varied in depth within the session such that five depths were presented of each S2 frequency. Subjects moved a joystick laterally to initiate a trial and were required to hold the joystick in that position for the duration of the trial until they moved the joystick up or down after S2 offset to indicate their response. Behavioral discrimination thresholds were defined as the point at which animals' average performance was 70% correct and were assessed for each animal after asymptotic performance on the task was reached. Subsequently, five AM depths were chosen such that two were near threshold, two were slightly above threshold and one was far above threshold.

Visual Task

After subjects had reached asymptotic performance on the auditory task, training in the visual modality began. Animals first were trained to fixate a dot (within a 2° fixation window), then to perform the auditory task while maintaining fixation throughout the duration of a trial. If fixation was lost at any point during the trial, the trial would be aborted and there would be a brief time out (1-2s). After they were consistently performing the auditory task with fixation, training on the visual task began.

Two, 400ms stochastic dot motion (SDM) videos were presented separated by a 400ms ISI and animals performed a dot motion direction discrimination task (Britten et al. 1992). The first stimulus was 100% coherent motion to the right, the second stimulus was motion of varied coherence either up or down. Animals had to report whether the motion in the S2 was up or down with a joystick movement either up or down. Visual discrimination thresholds were assessed as in the auditory task and five coherence levels were chosen such that two were near discrimination threshold, two were slightly above, and one was far above.

Intermodal Task

Once animals had reached asymptotic performance for the discrimination task in each modality, they began being presented with bimodal stimuli. Each bimodal block was preceded with a 60-trial unimodal block that served to cue the animal which modality to attend to in the upcoming bimodal block. Distracting stimuli were introduced sub-discrimination threshold and were gradually increased in detectability until the full range of stimuli could be presented and the animal could reliably perform the cued task while ignoring the distracting modality.

Since response direction was the same for both modalities, it was possible for the correct response to each modality to be the same on a bimodal trial (i.e., upward dot motion stimulus paired with a higher AM frequency stimulus where both response contingencies were for upward joystick motion), which we will define as “congruent” trials. These were equally balanced with “incongruent” trials in which the correct response for the two modalities of a bimodal stimulus were opposite. We also included a small proportion of “probe” trials, in which the S2 of the cued modality was either unmodulated broadband noise or 0% coherent dot motion, for auditory and vision respectively. Response contingencies were counterbalanced across subjects.

Stimuli

Auditory stimuli were created from broadband Gaussian (white) noise bursts (400ms; 5ms cosine ramped) that were 9 octaves in width (40Hz to 20480Hz). Four different seeds were used to create the carrier noise, which was frozen across trials. The noise envelope was then sinusoidally amplitude modulated (AM). Sound generation methods have been previously reported (O'Connor et al. 2011). In brief, sound signals were produced using an in-house MATLAB program and a digital-to-analog convertor (Cambridge Electronic Design (CED) model 1401). Signals were attenuated (TDT Systems PA5, Leader LAT-45), amplified (RadioShack MPS-200) and presented from a single speaker (***SONY SPEAKER INFO HERE), positioned approximately 1m in from of the subject, centered at the interaural midpoint. Sounds were generated at a 100kHz sampling rate. Intensity was calibrated to 65dB at the outer ear across all sounds (Bruel & Kjaer model 2231).

Visual stimuli were presented using an in-house MATLAB program and were presented using PsychophysicsToolbox (Brainard 1997). White dots on a grey background were presented full field, with a 2.1° exclusion window surrounding the fixation point. Dots were presented at a size of 0.2deg, density of 6 dots/degree^2 and velocity of 10deg/s.

The animal's eye position (right eye) was monitored using an infrared camera (model - XX) mounted to the right of the monitor. The video signal was fed to a PC running Oculomatic eye tracking software (Zimmermann et al. 2016), which determined the position of the animal's gaze on the monitor. A digital version of the eye position from Oculomatic was converted to an analog voltage signal (NI board, model XX) for input to the CED 1401 and recorded alongside the spiking data. The offset and gain of this eye position signal were calibrated prior to each recording session.

Analysis of firing rate-based neural discriminability

We used the signal detection theory-based metric, area under the receiver operating characteristic (ROCa), to measure how well neurons could discriminate AM (Green and Swets 1974). We assessed both how well neurons could discriminate AM sounds from the unmodulated carrier and how well the neurons could discriminate between the modulation frequencies. ROCa represents the probability that an ideal observer can discriminate between two stimuli given solely the neural responses. ROCa was calculated by separating the trial-by-trial neural responses into two distributions based on which AM frequency presented. Then, we determined the proportion of trials in each group where the neural response exceeded a criterion value. We repeated this measure using 100 criteria, covering the entire range of responses. The graph of the probability of exceeding criterion for the "high" frequency (or AM present) versus the "low" frequency (or unmodulated carrier) across all 100 criteria is the ROC. The area under this curve is the ROCa. ROCa is bounded by 0 and 1, where both extremes indicate perfect discrimination between the frequencies and 0.5 indicates chance level of discrimination. Cells that significantly discriminated AM noise from the unmodulated carrier at any depth were categorized as AM rate encoders. For assessing AM frequency discrimination, we reflected the ROCa about 0.5 such that our reflected-ROCa values were bounded by 0.5 and 1. Significance of this ROCa was assessed using a permutation test with 2000 repetitions.

Phase-Projected Vector Strength

Neural phase-locking to the stimulus was assessed using the metric phase-projected vector strength (VSpp). *VSpp* is a trial-based measure of synchrony that penalizes trial-based vector strength (VS) values if the mean phase of the trial is not aligned with the overall mean phase of the cell (Yin et al. 2011). Vector strength is defined as:

[Eq. 1]

$$VS = \frac{\sqrt{(\sum_{i=1}^{n} \cos \theta_i)^2 + (\sum_{i=1}^{n} \sin \theta_i)^2}}{n}$$

where *VS* is the vector strength, *n* is the number of spikes, and θ_i is the phase of each spike in radians, calculated by:

[Eq. 2]

$$\theta_i = 2\pi \frac{t_{i \, mod \, p}}{p}$$

where t_i is the time of the spike in ms relative to the onset of the stimulus and p is the period of the stimulus in ms (Goldberg and Brown 1969; Mardia and Jupp 2000). VSpp is calculated on a trial-by-trial basis and is defined as:

[Eq. 3]
$$VS_{pp} = VS_t \cos(\phi_t - \phi_c)$$

Where *VSpp* is phase-projected vector strength per trial, VS_t is the vector strength per trial (calculated as in equation 1), and φ_t and φ_c are the trial-by-trial and the mean phase angle in radians, respectively. These are calculated for each stimulus by:

[Eq. 4]
$$\phi = arctan2\left(\frac{\sum_{i=1}^{n}\sin\theta_i}{\sum_{i=1}^{n}\cos\theta_i}\right)$$

Where *n* is the number of spikes per trial (for φ_t) or over all trials (for φ_c) and arctan2 is a modified version of the arctangent that determines the correct quadrant of the output based on the signs of the cosine and sine inputs (MATLAB, *atan2*). Trials on which a cell fired no spikes was assigned a *VSpp* of zero.

Analysis of temporal-based discrimination

To evaluate how well neurons could discriminate AM frequencies by phase-locking, we created a VSpp- based classifier model. For each trial, three VSpp values were calculated: one for each of the AM frequencies presented in the session (the S1 or “mid” AM frequency, and the two S2 frequencies “high” and “low”). Then, the three VSpp values were compared and the spike train was classified as the identity with the greatest value. The classifier stimulus identity and actual stimulus identity were then compared and those in which the classifier was correct were labeled hits, while all others were labeled misses.

Analysis of choice-related activity

Choice-related activity was assessed by applying ROCa metrics as described for the firing rate-based discriminability of AM, except instead of separating trials by stimulus identity, we separated the trials by the animals’ behavioral response. This is referred to as choice probability, or CP (Britten et al. 1996). Firing rates were converted to z-scores for each stimulus, and then these z-scored rates were combined to assess choice-probability overall. Stimuli were included in the analysis if there were at least 5 responses in either direction (“higher” or “lower”), otherwise they were omitted from choice analyses.

Results

Rhesus macaques perform an audio-visual intermodal attention task

We designed a novel intermodal attention task in which subjects were presented with audio-visual stimuli and alternated blocks of performing a task in the auditory modality with blocks of performing a visual task (Figure 2.1). Values of auditory and visual stimuli were chosen such that the performance was approximately equivalent within a subject (Figure 2.2). The difficulty of each was matched in order to control for the level of attention required to complete the task. In trials where the distracting modality was incongruent, subjects predictably performed worse than the stimuli were congruent, however subjects generally performed reasonably well (Figure 2.2). Subjects were most likely to err when the target modality stimulus was near threshold and the distracting stimulus was far-above threshold (Figure 2.2).

Since stimulus levels (AM depth and % coherence) were chosen for each subject based on their psychophysical performance, the values of these levels were different between the two subjects. For the auditory stimuli, Monkey U was presented with AM depths of 10, 21, 43, 65 and 100 percent, and Monkey Q was presented with 21, 32, 43, 55 and 100 percent. For the visual stimuli, coherences of 4, 8, 16, 23 and 32 percent were presented to Monkey U, and coherences of 20, 50, 60, 70 100 percent were used for Monkey Q. For analyses in which the two subjects are combined, stimulus values are presented in ranked levels (1-5). All analyses were performed for each animal separately first, and upon verification that the two were not significantly different were pooled to increase statistical power.

Auditory neurons respond to attentional context

We recorded from 96 A1 neurons (43 from Monkey U, 53 from Monkey Q) and 106 ML neurons (54 from Monkey U, 52 from Monkey Q) while animals performed this task.

Approximately half of neurons in each area (51/96 in A1, 48/106 in ML) had firing rates that significantly differed by attended modality (2-way ANOVA, factor 1: auditory vs. visual, factor 2: unimodal vs. bimodal). Post-hoc analysis comparing the two bimodal conditions revealed that 40/96 cells in A1 and 38/106 in ML had a significant difference in firing rates ($p < 0.05$, Tukey-Kramer Multiple Comparisons

Test), indicating that firing rate differences were not simply driven by the absence of an auditory stimulus in the visual unimodal condition.

In fact, while many neurons had lower firing rates during the visual unimodal block, there were many cells that had an increased firing rate during the visual unimodal block compared to the auditory unimodal block. In A1, 21.9% of cells had a significantly greater firing rate in the visual than in the auditory unimodal block ($p < 0.05$, *t*-test). This effect was similar in ML, where 29.3% of cells had a significantly greater firing rate during the visual unimodal block than the auditory unimodal block ($p < 0.05$, *t*-test). These proportions are similar to the proportion of cells that had the opposite effect: a significantly greater firing rate during the auditory unimodal block than the visual. 20.8% of A1 cells and 23.6% of ML cells had an increased firing rate in the auditory unimodal block than the visual ($p<0.05$, *t*-test).

In addition to having an increased firing rate during the visual only trials, several of these cells were visually driven. We compared the stimulus driven firing rates to the spontaneous rates during the visual unimodal blocks and found that 8.3% of cells in A1 and 8.4% in ML had significantly greater driven rates than spontaneous ($p<.05$, t-test).

AM rate encoding differs between contexts

To assess how well neurons encoded AM, we first examined how well they could discriminate AM sounds from the unmodulated carrier using signal detection-based theory metric ROCa. Cells that significantly discriminated AM from unmodulated noise at any AM depth were classified as AM rate encoders. In A1 60/96 and in ML 50/106 cells were AM rate encoders. We then assessed how well AM rate coders could discriminate between the “high” and “low” AM frequencies in each attention condition. Surprisingly, there were slightly fewer cells that significantly discriminated AM frequencies at any depth during the auditory instruction block (14/96 A1, 20/106 ML) than either the attend auditory bimodal (24/96 A1, 26/106 ML) or attend visual bimodal conditions (27/96, 26/106 ML). However, when comparing discrimination between conditions for all AM coders, regardless of significant AM frequency discrimination, ROCa was significantly higher in the auditory instruction block than either of the bimodal conditions (Figure 2.3; $p < 0.05$ *t*-test). The two bimodal conditions were not significantly different except for in ML at the third AM depth, where the attend visual bimodal ROCa was significantly greater than the attend auditory bimodal (Figure 2.3 p = 0.0024, *t*-test).

Strength of visual distractor modulates AM encoding

To assess how the strength of the visual distracting stimulus affected AM encoding in the attend auditory bimodal context, we calculated AM discriminability with ROCa for the bimodal stimuli with highest and the lowest visual distractor strength (coherence rank 5 and 1, respectively) separately (Figure 2.5). We found that AM discrimination was significantly better when the visual distractor was weak than when it was strong at AM depths that were slightly above threshold (AM levels 2 and 3). For A1, the mean ROCa in the presence of the weak distractor for AM level 2 was 0.64, compared with 0.57 in the presence of the strong distractor (p = 0.0031, two-tailed t-test). This was similar at AM level 3 in A1 (strong distractor ROCa = 0.57, weak distractor ROCa = 0.65, p = 0.0073). It was not significantly different between the visual distractors when the AM depth was the weakest (AM level 1, strong distractor ROCa = 0.59, weak distractor ROCa = 0.58, p = 0.50) nor at the depths far above threshold (AM level 4, strong distractor ROCa = 0.68, weak distractor ROCa = 0.64, p = 0.16) for A1.

In ML there was also significantly better encoding for AM level 2 (strong distractor ROCa = 0.60, weak distractor ROCa = 0.64, p = 0.025) and AM level 3 (strong distractor ROCa = 0.61, weak distractor ROCa = 0.65, p = 0.008). For ML, there was not a difference between distractor strengths for AM level 1 (strong distractor ROCa = 0.62, weak distractor ROCa = 0.58, p = 0.14), however at AM level 4, there was a significant improvement in discrimination when the visual distractor was strong, compared to when it was weak (strong distractor ROCa = 0.71, weak distractor ROCa = 0.62, p = 0.015).

Synchronizing responses successfully discriminate modulation frequency

Before we assessed how well neurons could discriminate between AM frequencies with synchronizing responses, we classified cells as synchronizing or non-synchronizing by if they significantly discriminated any AM frequency from unmodulated noise. In A1, 72/96 of cells had synchronized responses to the stimulus. In ML, 52/106 cells significantly synchronized. We then analyzed how well the cells that synchronized responses could discriminate between AM frequency. To do this, we created a simple classifier model (Figure 2.5) where for each trial, we calculated the VSpp value for each of the three AM frequencies present in the session (“high” frequency, “low” frequency, and the S1 comparator “mid” frequency). These three VSpp values were then compared and the AM frequency with the strongest VSpp response was selected as the classified identity. The classified identity could then be compared to the actual identity of the stimulus to assess the accuracy of the measure.

Accuracy of the VSpp classifier was significantly greater than chance (0.33) for AM depths 1-4 during the auditory unimodal condition ($p<0.05$, one-sample t-test) in the synchronizing populations for A1 (Figure 2.7a; level 1 mean = 0.43, p = 5.3e-7; level 2 mean = 0.37, p = 0.035; level 3 mean = 0.39, p = 0.002; level 4 mean = 0.40, p = 4.9e-4). In the attend auditory bimodal condition, the A1 synchronizing population was significantly greater than chance at AM discrimination for AM levels 2 (mean = 0.39, p = 0.0012), 3 (mean = 0.36, p = 0.024), and 5 (mean = 0.39, p = 0.0011). Even fewer AM levels were greater than chance detection during the attend visual bimodal condition in A1, only AM depth level 3 (mean = 0.43, p = 1.2e-5) and level 5 (mean = 0.39, p = 9.4e-4). The ML synchronizing population, by contrast, was significantly greater than chance at VSpp classification for all AM depths in all three auditory-present conditions (Figure 2.7b).

Synchronizing responses differ between unimodal and bimodal contexts

In both A1 and ML, VSpp-based discrimination tended to be better during the unimodal auditory (A) context than during either the attend auditory bimodal (AV) or attend visual bimodal (VA) contexts (Figure 2.7). In A1, the unimodal context was significantly better than the attend auditory bimodal context for AM level 1 (A mean = 0.43, AV mean = 0.35, p = 3.4e-7, two-tailed t-test) and 4 (A mean = 0.40, AV mean = 0.33, p = 3.9e-5). The difference between the unimodal auditory and the attend visual bimodal conditions was somewhat greater, where the former was significantly better at AM discrimination for AM levels 1 (A mean = 0.43 , VA mean = 0.34, p = 2.8e-7), 2 (A mean = 0.37, VA mean = 0.34, p = 0.02), and 4 (A mean = 0.4 , VA mean =0.35 , p = 7.4e-4). The two bimodal contexts were more similar, with the attend auditory bimodal context encoding AM significantly greater than the attend visual bimodal context only for AM level 2 (AV mean = 0.39, VA mean = 0.34, p = 1.1e-5).

Surprisingly, the unimodal auditory context was significantly worse than both bimodal contexts at the greatest AM depth (A mean = 0.33, AV mean = 0.39, VA mean = 0.39, p = 0.004 A vs AV, p = 0.001 A vs VA). Additionally, the attend visual bimodal context significantly discriminated AM greater than both attend auditory contexts at AM level 3 (A mean = 0.39, AV mean = 0.36, VA mean = 0.43, p = 0.01 VA vs A, p = 5.3e-6 VA vs AV).

There was a similar encoding advantage in the unimodal auditory context over the bimodal contexts in ML synchronizing neurons. In the unimodal auditory condition neurons discriminated AM significantly better than during the attend auditory bimodal context for AM level 1 (A mean = 0.47, AV mean = 0.40, p = 7.9e-7), 2 (A mean = 0.46, AV mean = 0.44, p = 0.03), and 4 (A mean = 0.46, AV mean = 0.42, p = 0.006). The effect was similar in between the unimodal auditory and the attend visual bimodal contexts where the encoding was significantly better in the unimodal attend auditory condition for AM levels 1 (A mean = 0.47, VA mean = 0.40, p = 3.5e-6), 2 (A mean = 0.26, VA mean = 0.40, p = 7.2e-4), and 4 (A mean = 0.46, VA mean = 0.43, p = 0.02). There was no significant difference in encoding between any of the three contexts for the most salient AM depth (level 5). As in A1, encoding was significantly better during the attend visual bimodal context than either the unimodal auditory or the auditory bimodal context for AM level 3 (A mean = 0.40, AV mean = 0.42, VA mean = 0.47, VA vs. A p = 2.4e-5, VA vs. AV p = 2.6e-5). Further, the attend auditory bimodal context was only significantly better than the attend visual bimodal context at discriminating AM level 2 (AV mean = 0.44, VA mean = 0.40, p = 0.009).

ML synchronizing responses discriminate AM better than A1 during bimodal contexts

While A1 had a significantly larger population of neurons that had synchronizing responses than ML (χ^2 = 5.52, p = 0.02), the ML synchronizing neurons were better at AM discrimination than the A1 synchronizing neurons in almost all bimodal contexts. In the attend auditory bimodal context, ML was significantly better than A1 at all AM levels ($p < 0.05$ for all levels, two sample t-test). In the attend visual bimodal context, ML had significant better encoding that A1 for all except AM level 3, where there was no significant difference between the two. There was less of a difference between the two areas in the auditory unimodal condition, where only AM levels 2, 4 and 5 were encoded significantly better in ML than A1 synchronizing neurons.

Choice-related activity varies with context

We found a subset of cells in both A1 and ML that had neural activity correlated with the animals' behavioral choice. When choice-related activity was compared between attentional contexts during the response epoch (after stimulus offset, before joystick movement report), choice-related activity was the weakest during the unimodal auditory context surprisingly in both A1 (population mean CP = 0.50, Figure 2.8) and ML (population mean CP = 0.51, Figure 2.8), which corresponded with the fewest individual neurons with significant choice-related activity of any condition (17.7% A1 neurons, 19.9% ML neurons). There were about twice as many neurons with significant choice-related activity during both the attend auditory bimodal context (39.6% of A1 neurons, 36.8% of ML neurons) and the attend visual bimodal context (45.8% of A1 neurons, 35.8% of ML neurons). Correspondingly, the average population choice-related activity was significantly different from chance in both bimodal contexts for A1 (attend auditory mean CP = 0.46, p = 1.2e-6, two-tailed t-test; attend visual mean CP = 0.44, p = 2.6e-11) and ML (attend auditory mean CP = 0.45, p = 4.7e-10; attend visual mean CP = 0.44, p = 9.5e-12). In ML, the mean CP was not significantly different between the two bimodal contexts (p = 0.07, two-tailed t-test). Though in A1, choice-related activity was significantly stronger during the attend visual bimodal context than the attend auditory (p = 6.4e-4). Unexpectedly, we found choice-related activity during the visual unimodal condition was similar to the two bimodal contexts both in the proportion of cells with significant choice-related activity (35.4% of A1 neurons, 36.8% of ML neurons) and the average population CP values (A1 mean CP = 0.46, ML mean CP = 0.47, Figure 2.8).

For all attentional contexts, there was less choice-related activity during the stimulus epoch than during the response epoch (Figure 2.8). In A1, during the auditory unimodal context, 10.4% of neurons had significant choice-related activity. In the attend auditory bimodal context 12.5% of neurons had significant choice activity, whereas only 6.3% of neurons had significant choice-related activity during the attend visual bimodal context. During the visual unimodal context, 9.4% of neurons had significant choice related activity. For all contexts, the population averages were not significantly different from chance (p >

0.05, two-tailed t-test). This was similar in ML, where 12.3% of neurons had significant choice-related activity during the auditory unimodal condition, 11.3% during the attend auditory bimodal context, 10.4% during the attend visual bimodal context and 11.3% during the visual unimodal context. This also corresponded with population averaged choice activity that was not significantly different from chance (Figure 2.8).

Choice-related activity and stimulus congruency

We then assessed how stimulus congruency affected choice-related activity by calculating CP values separately for congruent and incongruent trials (Figure 2.9). We found that during the response epoch, in A1, there was not a significant difference between congruent and incongruent trials in either the attend auditory condition (congruent mean CP = 0.46, incongruent mean CP = 0.46, $p = 6.2$, two-tailed t-test) or the attend visual condition (congruent mean CP = 0.44, incongruent mean CP = 0.44, $p = 0.72$). In ML however, there was a significantly stronger choice-related activity on congruent than incongruent trials in both the attend auditory condition (congruent mean CP = 0.45, incongruent mean = 0.47, $p = 0.0011$) and the attend visual condition (congruent mean CP = 0.44, incongruent mean = 0.46, $p = 0.029$).

During the stimulus window, there were no significant differences between the congruent and incongruent trials in A1 during either the attend auditory (congruent mean CP = 0.50, incongruent mean CP = 0.50, $p = 0.28$) or the attend visual (congruent mean CP = 0.50, incongruent mean CP = 0.50, $p = 0.97$) conditions (Figure 2.9). This was similar in ML where neither the attend auditory (congruent mean CP = 0.51, incongruent mean CP = 0.51, $p = 0.66$) nor the attend visual (congruent mean CP = 0.49, incongruent mean CP = 0.49, $p = 0.28$) contexts differed significantly based on the congruency of the auditory and visual stimulus (Figure 2.9).

Discussion

We found a large population of neurons in both A1 and ML had significantly different firing rates between attentional contexts. However, of these context dependent cells, only about half of them significantly encoded AM. This context-dependent change in firing rate is consistent with results from Scott and colleagues who found behavioral context induced large-scale changes in activity that was not accompanied with an increase in encoding both in auditory cortex (Scott et al. 2007). There was also a subset of cells that had significantly higher firing rates during the visual unimodal context than the auditory unimodal context. This is consistent with findings from Brosch and colleagues who found in an auditory-visual intermodal task most of the multi-unit activity had increased firing rates during the visual task (Brosch et al. 2015). Further, some of these cells had responses that were driven by the visual stimulus, rather than just overall increased excitability. This extends upon previously reported effects of non-auditory task relevant responses in auditory cortex (Bizley and King 2009; Brosch 2005; Kayser et al. 2005, 2008; Maddox et al. 2015). Visual responses previously reported are typically modulatory and have been hypothesized to help with things such as audiovisual integration and sound source localization (Bizley and King 2009; Ghazanfar 2005; Maddox et al. 2015).

For both rate- and temporal- based encoding of AM, neurons were better during the auditory unimodal block than in either of the bimodal contexts. However, there was little difference in the encoding between the attend auditory bimodal context and the attend visual bimodal context. This suggests that the presence of the distracting stimulus worsened AM encoding, whereas attending to the visual stimulus over the auditory did not significantly affect AM encoding at the single neuron level. This theory was further supported when we compared the discriminability of AM when the distracting visual stimulus was strong (coherence level 5) to when it was weak (coherence level 1). There was a significant improvement in AM discriminability in the presence of the weak distractor for the AM depths slightly above threshold (AM levels 2 and 3).

Consistent with previous reports, we found fewer neurons in ML than A1 with responses that synchronized with AM stimuli. However, surprisingly, ML synchronizing neurons discriminated AM significantly better than the A1 synchronizing neurons. It has been shown that AM encoding transitions from a primarily temporal code at lower levels of auditory processing to a primarily rate code as the information is passed through auditory cortex, with fewer neurons phase-locking responses, as well as generally weaker phase-locking at higher areas (Johnson et al. 2020; Joris et al. 2004; Niwa et al. 2013, 2015). However, in a recent study comparing AM encoding between A1 and ML found that ML neurons tended to be slightly more broadly tuned to AM frequency with VSpp responses (Johnson et al. 2020), which could help explain the results here. It’s possible that ML synchronizing neurons temporally encoded *both* the “high” and “low” frequency stimuli, whereas in A1, the narrower AM frequency tuning it only synchronized responses to one of the AM frequencies, thus impacting temporal-based discrimination.

We observed a large subset of cells with choice-related activity during the response epoch in both A1 and ML, and a smaller subset of cells with choice-related activity during the stimulus window, consistent with previous reports (Bizley et al. 2013; Guo et al. 2019; Niwa et al. 2013). We were surprised to find that choice-related activity was the weakest during the auditory unimodal condition than either of the bimodal conditions or even the visual unimodal condition. This suggests that the visual-choice is reflected in the auditory cortex, perhaps even more-so than the auditory choice. We expect that visual decision-related activity seen here is an effect of training on this bimodal task. Further, we found that the congruency of the bimodal stimulus effected choice-related activity in ML, where choice activity was stronger on congruent trials than incongruent. We posit that this reflects a modulation of choice-related activity by reward expectation, or what in human literature could be called confidence. On incongruent trials, the conflicting audio-visual information causes the animal to have a lower expectation of reward than when the information is congruent. This would be consistent with reports from others who have found neural activity modulated by reward expectation (Brosch et al. 2011; David et al. 2012; Guo et al. 2019). For example, in one study where they manipulated reward size while mice performed a sound discrimination task (Guo et al. 2019), they found that reward expectation modulated responses in a large proportion of choice-selective neurons, more so than even the stimulus selective neurons. We believe our results support a similar consequence of reward expectation, however further studies systematically manipulating reward expectation in the context of bimodal stimuli are necessary.

In summary, while many cells in both A1 and ML changed their firing rate based on the attended modality, changes in task-relevant stimulus encoding were largely modulated by the presence of a distracting stimulus. Improvements in AM frequency encoding – both rate- and temporally-based – were seen when the auditory stimulus was presented alone, compared to audio-visual stimulus presentations. Finally, the presence of a small subset of cells in both A1 and ML that were driven by visual stimuli alone suggests that cross-modal influences in auditory cortex could play more than simply a modulatory role in auditory cortex.

References

Bagur S, **Averseng M**, **Elgueda D**, **David S**, **Fritz J**, **Yin P**, **Shamma S**, **Boubenec Y**, **Ostojic S**. Go/No-Go task engagement enhances population representation of target stimuli in primary auditory cortex. *Nat Commun* 9: 2529, 2018.

Bizley JK, **King AJ**. Visual influences on ferret auditory cortex. *Hearing Research* 258: 55–63, 2009.

Bizley JK, **Walker KMM**, **Nodal FR**, **King AJ**, **Schnupp JWH**. Auditory Cortex Represents Both Pitch Judgments and the Corresponding Acoustic Cues. *Current Biology* 23: 620–625, 2013.

Brainard DH. The Psychophysics Toolbox. *Spatial Vis* 10: 433–436, 1997.

Britten K, **Shadlen M**, **Newsome W**, **Movshon J**. The analysis of visual motion: a comparison of neuronal and psychophysical performance. *The Journal of Neuroscience* 12: 4745–4765, 1992.

Britten KH, **Newsome WT**, **Shadlen MN**, **Celebrini S**, **Movshon JA**. A relationship between behavioral choice and the visual responses of neurons in macaque MT. *Visual Neuroscience* 13: 87–100, 1996.

Brosch M. Nonauditory Events of a Behavioral Procedure Activate Auditory Cortex of Highly Trained Monkeys. *Journal of Neuroscience* 25: 6797–6806, 2005.

Brosch M, **Selezneva E**, **Scheich H**. Representation of Reward Feedback in Primate Auditory Cortex. *Frontiers in Systems Neuroscience* 5, 2011.

Brosch M, **Selezneva E**, **Scheich H**. Neuronal activity in primate auditory cortex during the performance of audiovisual tasks. *European Journal of Neuroscience* 41: 603–614, 2015.

Cohen MR, **Maunsell JHR**. Using Neuronal Populations to Study the Mechanisms Underlying Spatial and Feature Attention. *Neuron* 70: 1192–1204, 2011.

David SV, **Fritz JB**, **Shamma SA**. Task reward structure shapes rapid receptive field plasticity in auditory cortex. *Proceedings of the National Academy of Sciences* 109: 2144–2149, 2012.

Desimone R, **Duncan J**. Neural Mechanisms of Selective Visual Attention. *Annual Review of Neuroscience* 18: 193–222, 1995.

Downer JD, **Niwa M**, **Sutter ML**. Task Engagement Selectively Modulates Neural Correlations in Primary Auditory Cortex. *Journal of Neuroscience* 35: 7565–7574, 2015.

Downer JD, **Rapone B**, **Verhein J**, **O'Connor KN**, **Sutter ML**. Feature-Selective Attention Adaptively Shifts Noise Correlations in Primary Auditory Cortex. *The Journal of Neuroscience* 37: 5378–5392, 2017.

Francis NA, **Winkowski DE**, **Sheikhattar A**, **Armengol K**, **Babadi B**, **Kanold PO**. Small Networks Encode Decision-Making in Primary Auditory Cortex. *Neuron* 97: 885-897.e6, 2018.

Fritz JB, **Elhilali M**, **Shamma SA**. Adaptive Changes in Cortical Receptive Fields Induced by Attention to Complex Sounds. *Journal of Neurophysiology* 98: 2337–2346, 2007.

Ghazanfar AA. Multisensory Integration of Dynamic Faces and Voices in Rhesus Monkey Auditory Cortex. *Journal of Neuroscience* 25: 5004–5012, 2005.

Goldberg JM, **Brown PB**. Response of binaural neurons of dog superior olivary complex to dichotic tonal stimuli: some physiological mechanisms of sound localization. *Journal of Neurophysiology* 32: 613–636, 1969.

Green DM, **Swets JA**. *Signal detection theory and psychophysics*. Huntington, NY: Krieger Publishing Company, 1974.

Guo L, **Weems JT**, **Walker WI**, **Levichev A**, **Jaramillo S**. Choice-Selective Neurons in the Auditory Cortex and in Its Striatal Target Encode Reward Expectation. *J Neurosci* 39: 3687–3697, 2019.

Hartmann T, **Weisz N**. Auditory cortical generators of the Frequency Following Response are modulated by intermodal attention. *NeuroImage* 203: 116185, 2019.

Hocherman S, **Benson DA**, **Goldstein MH**, **Heffner HE**, **Hienz RD**. Evoked unit activity in auditory cortex of monkeys performing a selective attention task. *Brain Research* 117: 51–68, 1976.

Johnson JS, **Niwa M**, **O'Connor KN**, **Sutter ML**. Amplitude modulation encoding in the auditory cortex: comparisons between the primary and middle lateral belt regions. *Journal of Neurophysiology* 124: 1706–1726, 2020.

Joris PX, **Schreiner CE**, **Rees A**. Neural Processing of Amplitude-Modulated Sounds. *Physiological Reviews* 84: 541–577, 2004.

Karns CM, **Knight RT**. Intermodal Auditory, Visual, and Tactile Attention Modulates Early Stages of Neural Processing. *Journal of Cognitive Neuroscience* 21: 669–683, 2009.

Kayser C, **Petkov CI**, **Augath M**, **Logothetis NK**. Integration of Touch and Sound in Auditory Cortex. *Neuron* 48: 373–384, 2005.

Kayser C, **Petkov CI**, **Logothetis NK**. Visual Modulation of Neurons in Auditory Cortex. *Cerebral Cortex* 18: 1560–1574, 2008.

Lemus L, **Hernández A**, **Luna R**, **Zainos A**, **Romo R**. Do Sensory Cortices Process More than One Sensory Modality during Perceptual Judgments? *Neuron* 67: 335–348, 2010.

Maddox RK, **Atilgan H**, **Bizley JK**, **Lee AK**. Auditory selective attention is enhanced by a task-irrelevant temporally coherent visual stimulus in human listeners. *eLife* 4, 2015.

Mardia KV, **Jupp PE**. *Directional statistics*. Chichester; New York: J. Wiley, 2000.

Maunsell JHR. Neuronal Mechanisms of Visual Attention. *Annual Review of Vision Science* 1: 373–391, 2015.

Maunsell JHR, **Cook EP**. The role of attention in visual processing. *Phil Trans R Soc Lond B* 357: 1063–1072, 2002.

Mehta AD. Intermodal Selective Attention in Monkeys. I: Distribution and Timing of Effects across Visual Areas. *Cerebral Cortex* 10: 343–358, 2000a.

Mehta AD. Intermodal Selective Attention in Monkeys. II: Physiological Mechanisms of Modulation. *Cerebral Cortex* 10: 359–370, 2000b.

Merzenich MM, **Brugge JF**. Representation of the cochlear partition on the superior temporal plane of the macaque monkey. *Brain Research* 50: 275–296, 1973.

Mirabella G, **Bertini G**, **Samengo I**, **Kilavik BE**, **Frilli D**, **Della Libera C**, **Chelazzi L**. Neurons in Area V4 of the Macaque Translate Attended Visual Features into Behaviorally Relevant Categories. *Neuron* 54: 303–318, 2007.

Ni AM, **Maunsell JHR**. Neuronal Effects of Spatial and Feature Attention Differ Due to Normalization. *J Neurosci* 39: 5493–5505, 2019.

Niwa M, **Johnson JS**, **O'Connor KN**, **Sutter ML**. Active Engagement Improves Primary Auditory Cortical Neurons' Ability to Discriminate Temporal Modulation. *Journal of Neuroscience* 32: 9323–9334, 2012a.

Niwa M, **Johnson JS**, **O'Connor KN**, **Sutter ML**. Activity Related to Perceptual Judgment and Action in Primary Auditory Cortex. *Journal of Neuroscience* 32: 3193–3210, 2012b.

Niwa M, **Johnson JS**, **O'Connor KN**, **Sutter ML**. Differences between Primary Auditory Cortex and Auditory Belt Related to Encoding and Choice for AM Sounds. *Journal of Neuroscience* 33: 8378–8395, 2013.

Niwa M, **O'Connor KN**, **Engall E**, **Johnson JS**, **Sutter ML**. Hierarchical effects of task engagement on amplitude modulation encoding in auditory cortex. *Journal of Neurophysiology* 113: 307–327, 2015.

O'Connell MN, **Barczak A**, **Schroeder CE**, **Lakatos P**. Layer Specific Sharpening of Frequency Tuning by Selective Attention in Primary Auditory Cortex. *The Journal of Neuroscience* 34: 16496–16508, 2014.

O'Connor KN, **Johnson JS**, **Niwa M**, **Noriega NC**, **Marshall EA**, **Sutter ML**. Amplitude modulation detection as a function of modulation frequency and stimulus duration: Comparisons between macaques and humans. *Hearing Research* 277: 37–43, 2011.

Otazu GH, **Tai L-H**, **Yang Y**, **Zador AM**. Engaging in an auditory task suppresses responses in auditory cortex. *Nature Neuroscience* 12: 646–654, 2009.

Rauschecker JP, **Tian B**. Processing of Band-Passed Noise in the Lateral Auditory Belt Cortex of the Rhesus Monkey. *Journal of Neurophysiology* 91: 2578–2589, 2004.

Rodgers CC, **DeWeese MR**. Neural Correlates of Task Switching in Prefrontal Cortex and Primary Auditory Cortex in a Novel Stimulus Selection Task for Rodents. *Neuron* 82: 1157–1170, 2014.

Saleem K, **Logothetis Nikos K**. *A combined MRI and histology atlas of the rhesus monkey brain in sterotaxic coordinates*. Burlington, MA: Academic Press, 2007.

Saupe K. Neural mechanisms of intermodal sustained selective attention with concurrently presented auditory and visual stimuli. *Frontiers in Human Neuroscience* 3, 2009.

Saupe K, **Widmann A**, **Bendixen A**, **Müller MM**, **Schröger E**. Effects of intermodal attention on the auditory steady-state response and the event-related potential. *Psychophysiology* 46: 321–327, 2009.

Schwartz ZP, **David SV**. Focal Suppression of Distractor Sounds by Selective Attention in Auditory Cortex. *Cerebral Cortex* 28: 323–339, 2018.

Scott BH, **Malone BJ**, **Semple MN**. Effect of Behavioral Context on Representation of a Spatial Cue in Core Auditory Cortex of Awake Macaques. *Journal of Neuroscience* 27: 6489–6499, 2007.

Stoilova VV, **Knauer B**, **Berg S**, **Rieber E**, **Jäkel F**, **Stüttgen MC**. Auditory cortex reflects goal-directed movement but is not necessary for behavioral adaptation in sound-cued reward tracking. *Journal of Neurophysiology* 124: 1056–1071, 2020.

Tian B, **Rauschecker JP**. Processing of Frequency-Modulated Sounds in the Lateral Auditory Belt Cortex of the Rhesus Monkey. *Journal of Neurophysiology* 92: 2993–3013, 2004.

Tsunada J, **Liu ASK**, **Gold JI**, **Cohen YE**. Causal contribution of primate auditory cortex to auditory perceptual decision-making. *Nature Neuroscience* 19: 135–142, 2016.

Wimmer RD, **Schmitt LI**, **Davidson TJ**, **Nakajima M**, **Deisseroth K**, **Halassa MM**. Thalamic control of sensory selection in divided attention. *Nature* 526: 705–709, 2015.

Yin P, **Johnson JS**, **O'Connor KN**, **Sutter ML**. Coding of Amplitude Modulation in Primary Auditory Cortex. *Journal of Neurophysiology* 105: 582–600, 2011.

Zimmermann J, **Vazquez Y**, **Glimcher PW**, **Pesaran B**, **Louie K**. Oculomatic : High speed, reliable, and accurate open-source eye tracking for humans and non-human primates. *Journal of Neuroscience Methods* 270: 138–146, 2016.

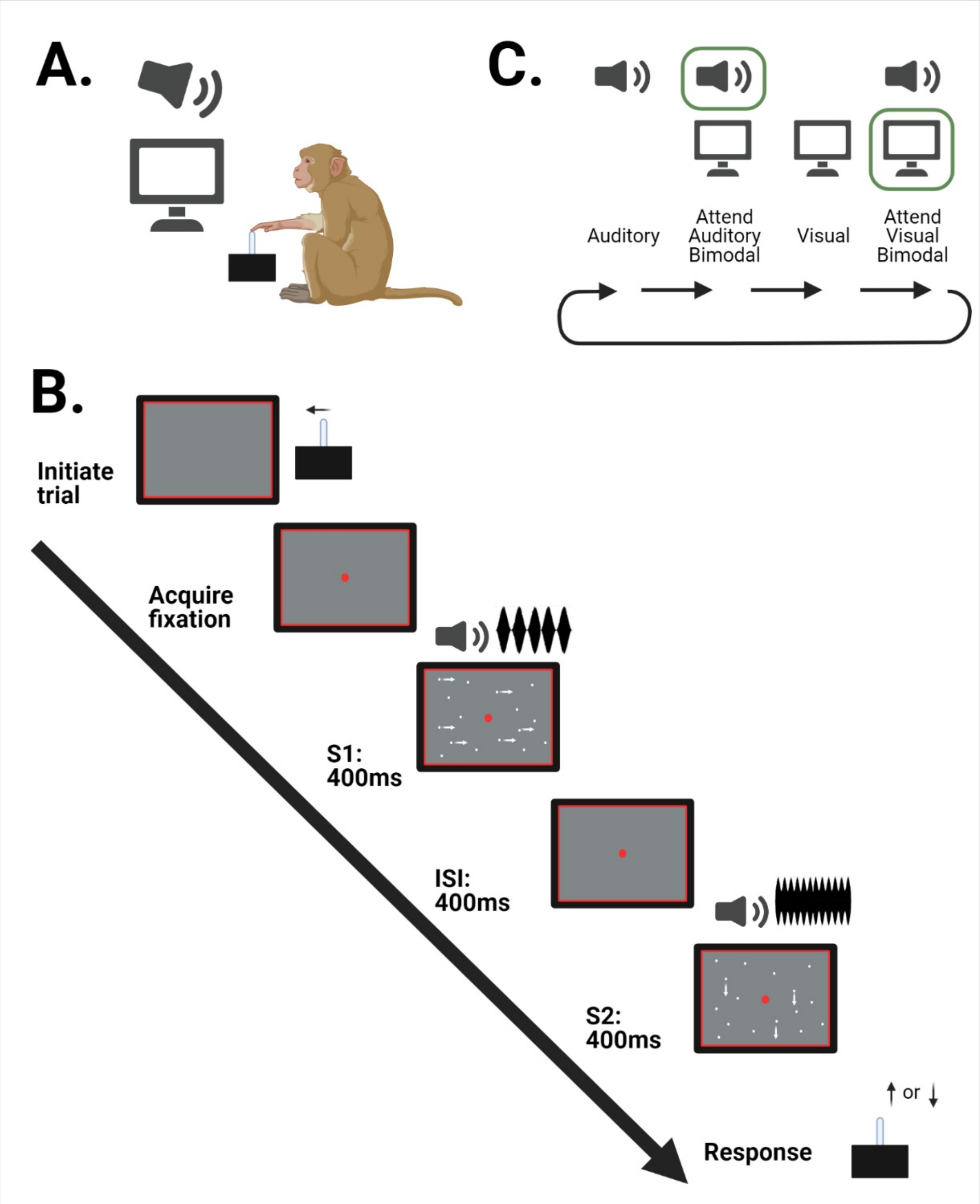

Figure 2.1 Intermodal Attention Task structure. **A.** Monkeys were placed in a sound booth with a joystick, a monitor was in front of them at eye level, a speaker was mounted above the monitor and angled towards the animal. **B.** Trial structure. Example is showing a bimodal trial. Each bimodal block was preceded by a unimodal block that cued the animal which modality to attend to in the bimodal block that followed. Fixation was still required during unimodal auditory blocks. **C.** Structure of attentional blocks within a session.

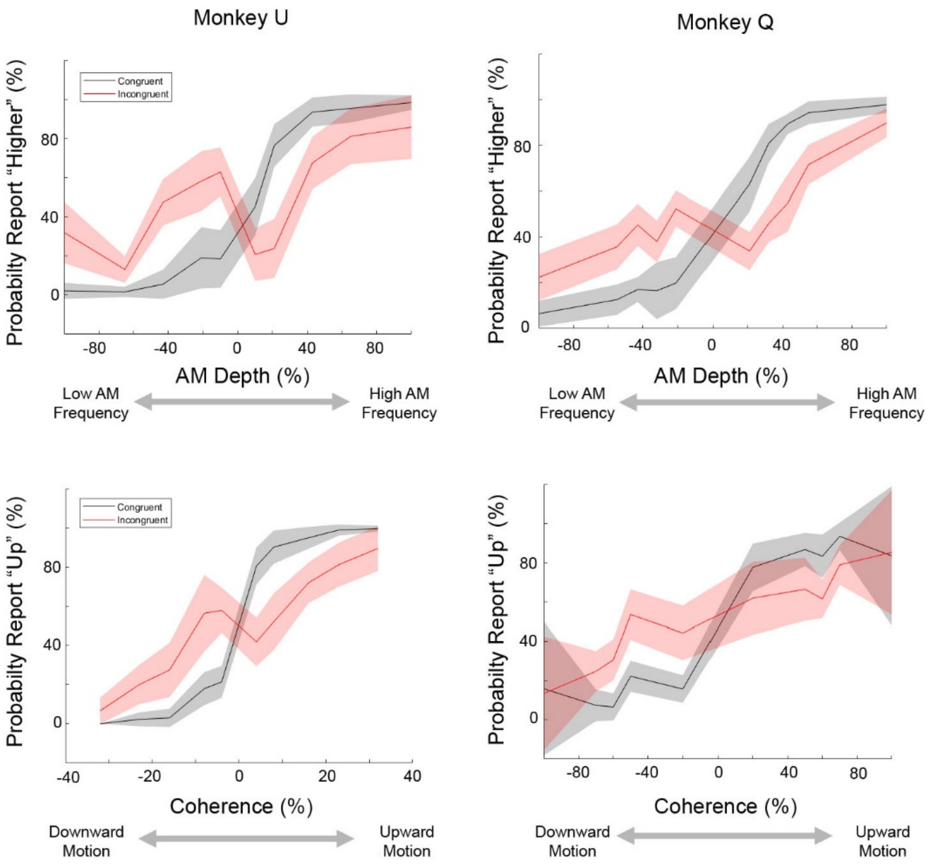

Figure 2.2 Average behavioral performance of each subject on the auditory (top) and visual (bottom) intermodal task. Performance was comparable between subjects on both tasks. While performance was expectedly worse on incongruent trials than congruent trials, they still typically responded primarily to the appropriate modality on incongruent trials.

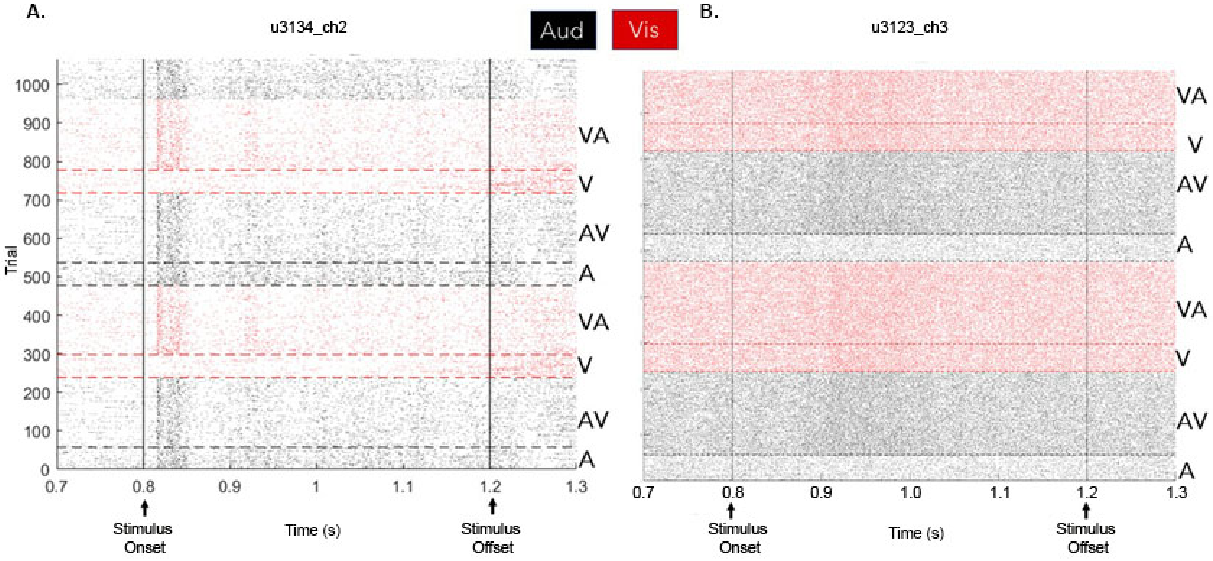

Figure 2.3 Example cells showing an effect of context on the firing rate. **(A)** shows an example cell with a significant context effect where auditory unimodal activity was greater than visual unimodal activity **(B)** shows a significant context effect where visual unimodal activity was greater than auditory unimodal activity.

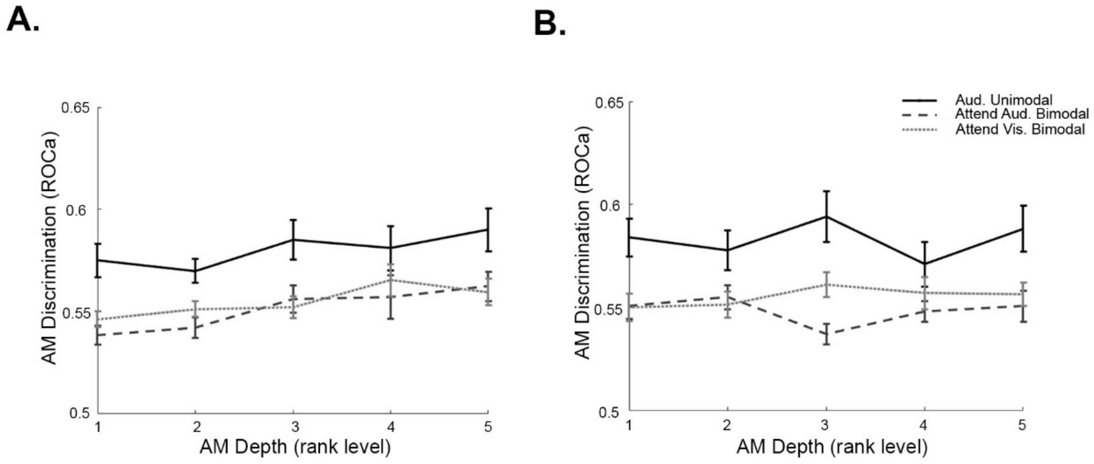

Figure 2.4 Firing rate-based AM frequency discrimination in **(A)** A1 rate encoders (n = 60) and **(B)** ML (n = 50) by attentional context. Discrimination of AM frequency was significantly greater during the unimodal auditory context than in either of the bimodal contexts.

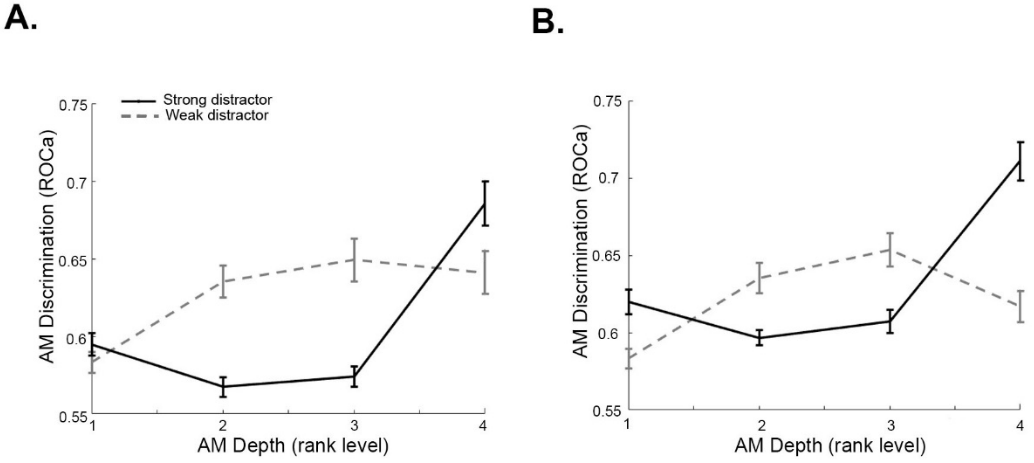

Figure 2.5 AM rate-based discrimination during attend auditory bimodal condition in the presence of a strong distracting visual stimulus (solid lines, visual rank 5) and a weak visual distractor (dashed lines, visual rank 1). Both A1 **(A)** and ML **(B)** neurons had significantly improved AM discrimination in the presence of the weak distractor (coherence rank 1) compared with the strong distractor (coherence rank 5) for AM depths slightly above threshold.

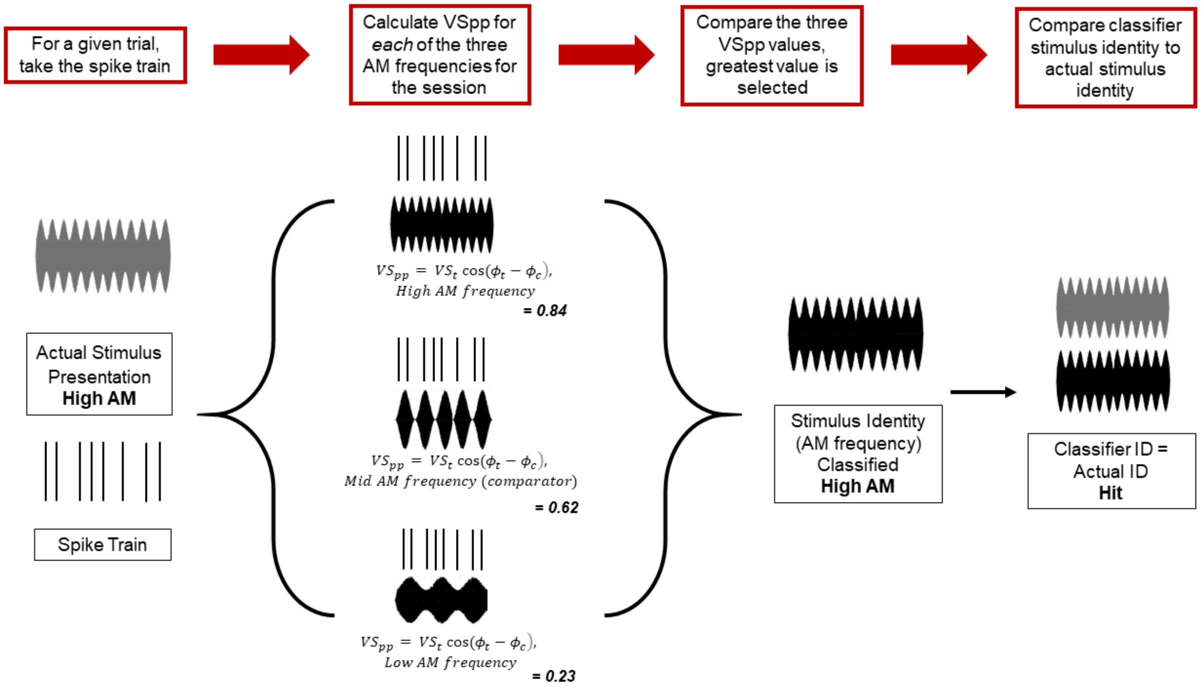

Figure 2.6 Schematic of VSpp-based AM frequency discrimination classifier. For a given trial, the phase projected vector strength is calculated for each of the AM frequencies used in the session (the S1 or “mid” AM frequency, “high” and “low”). The modulation frequency that calculates the highest VSpp value is then selected as the classified AM frequency identity. If the classifier identity is the same as the actual stimulus identity, it is a hit, otherwise it is a miss. This was repeated for every trial.

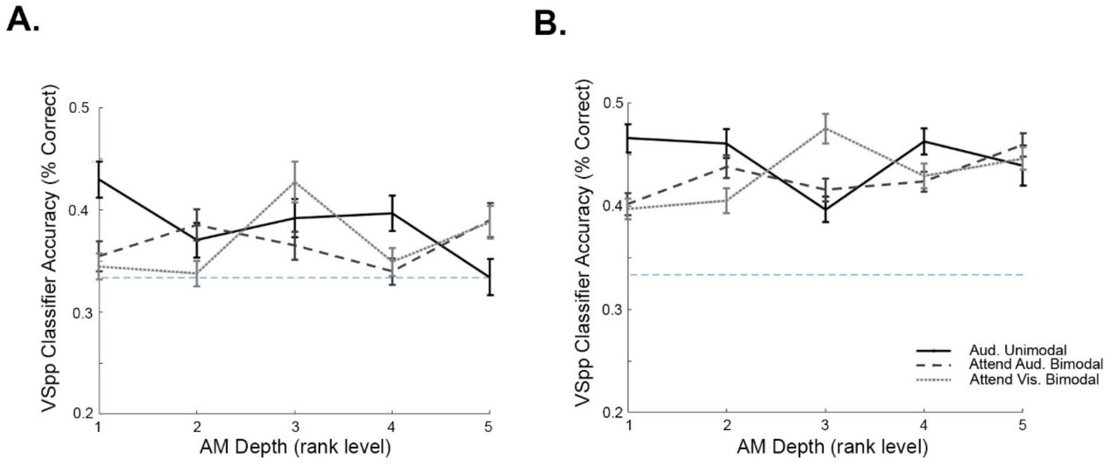

Figure 2.7 VSpp-based AM frequency discrimination in **(A)** A1 synchronizing neurons (n = 72) and ML **(B)** ML synchronizing neurons (n = 52). AM discrimination was better during the unimodal auditory context than either bimodal context for most AM depths.

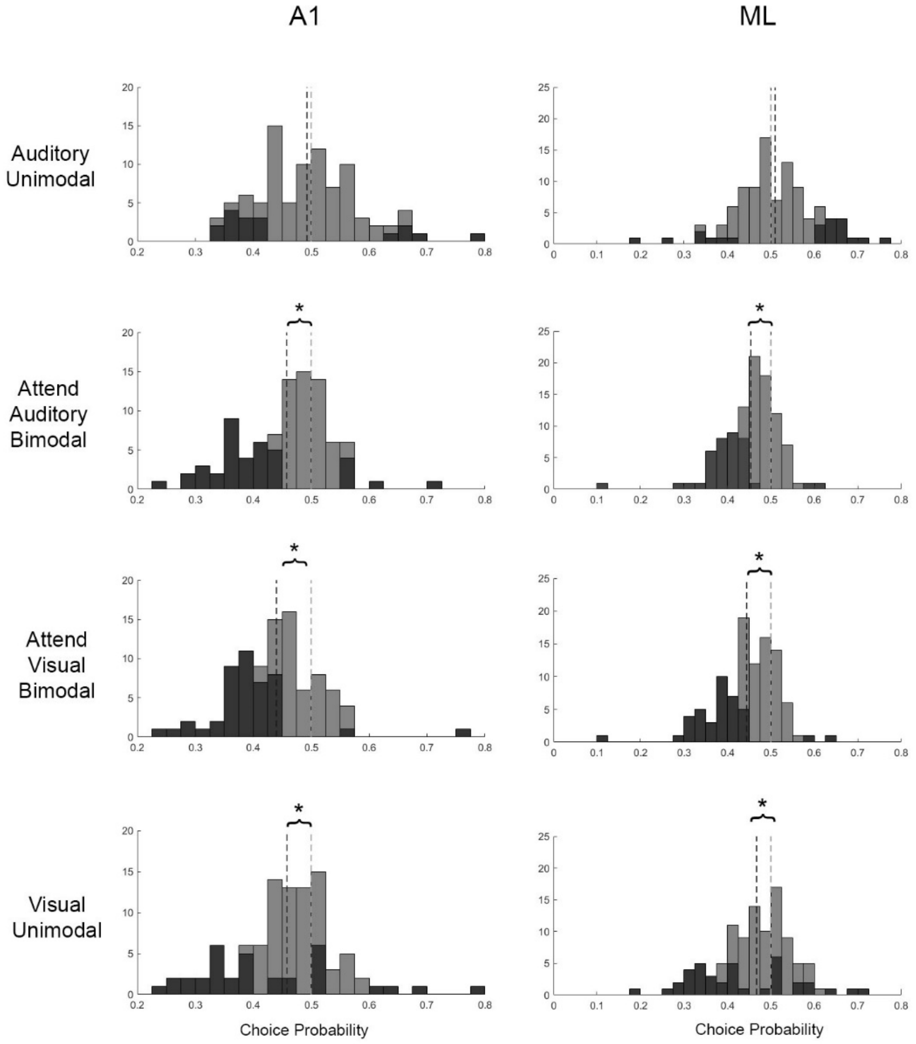

Figure 2.8 Choice related activity between contexts for A1 (left) and ML (right) during the response epoch. Light grey lines indicate 0.5, dark grey lines indicate population mean CP values. Population means significantly different than 0.5 for both A1 and ML in all conditions except for the attend auditory unimodal condition.

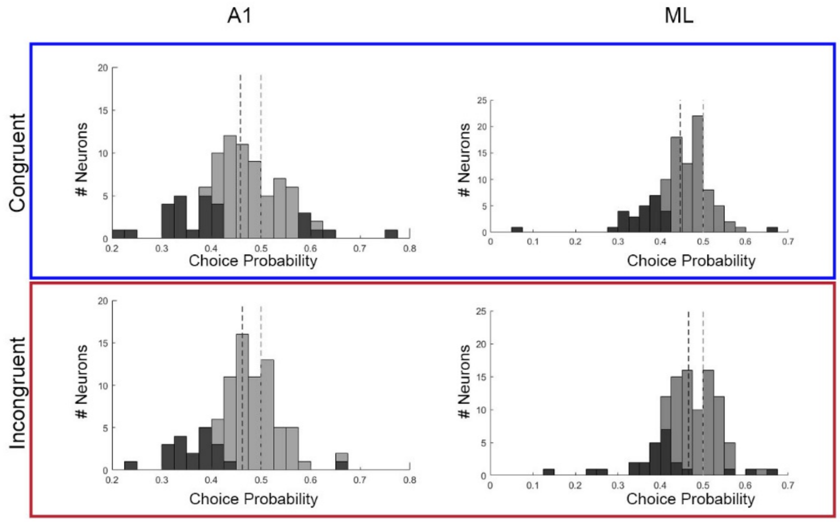

Figure 2.9 Choice related activity on congruent (top) and incongruent (bottom) trials. Light grey lines denote 0.5, dark grey lines indicate population mean CP values. In ML (right) choice probability was significantly better on congruent trials (mean CP = 0.45) than incongruent trials (mean CP = 0.47). In A1 (left) there was not a significant difference between congruent (mean CP = 0.46) and incongruent (mean CP = 0.46) trials.

General Discussion

The studies that comprise this dissertation aimed to disentangle general arousal effects from more specific effects of selectively attention. This addresses a gap in knowledge in the auditory cortex, where studies of attention at the single neuron level have largely utilized passive/active task paradigms to examine the effects of task engagement on cortical activity (Atiani et al. 2014; Bagur et al. 2018; Buran et al. 2014; Downer et al. 2015; Lee and Middlebrooks 2011; Niwa et al. 2012a). We examined how two different types of selective attention – feature-selective attention and intermodal attention – effect the encoding of amplitude modulation (AM) in auditory cortex. Previous studies have found that task engagement increases AM detection in single neurons in both primary (A1) and secondary (middle-lateral belt, ML) auditory cortex of Rhesus macaques (Niwa et al. 2012a, 2015). Task engagement has also been shown to modulate tuning properties (Fritz et al. 2003, 2007; Lin et al. 2019; Middlebrooks et al. 1980; Yin et al. 2014), alter firing rates (Miller et al. 1972) and modulate interneuronal correlated variability (Downer et al. 2015).

In the studies presented here, we found little evidence for improved encoding of AM noise with selective attention. During feature-selective attention, we did not find a change in either rate- or temporal-based AM detection when subjects attended to changes in AM compared with when they attended to changes in the spectral content of the carrier. Similarly, during the intermodal attention task, we did not find changes in AM frequency discrimination when animals attended to the auditory stimulus (and ignored the visual stimulus), compared to when subjects attended the visual stimulus and ignored the auditory. This was surprising, as we had expected to find increased discriminability of AM when it was attended to, as has been reported during task engagement (Atiani et al. 2014; Bagur et al. 2018; Carcea et al. 2017; Niwa et al. 2012a, 2015). Similarly, in the visual cortex where selective attention has been studied more frequently, increased discriminability in the form of gain changes have been reported (Martinez-Trujillo and Treue 2004; Ni and Maunsell 2019; Treue and Trujillo 1999). However, our findings suggest that selective attention in auditory cortex may employ different mechanisms than increased discriminability on the single neuron level. It is possible that in auditory cortex, attention modulates activity on the scale of populations of neurons. In a study examining interneuronal correlated variability using the same dataset of A1 cells from chapter one of this dissertation, Downer and colleagues found that feature-selective attention adaptively shifted correlated variability within pairs of neurons that had opposite feature-specific tuning (Downer et al. 2017b). This supports the idea that selective attention may act on the level of small populations of neurons in auditory cortex.

The one context in which we did find an effect of attention at the level of the single neuron was between the unimodal and bimodal conditions in the intermodal attention experiment. AM discrimination was significantly improved during the unimodal auditory context compared with either of the bimodal contexts. This, along with the lack of difference between the two bimodal attentional conditions, suggests that the differences we report here are likely due to the effect of the presence of a distracting stimulus. This was further supported by AM discrimination being better when the distracting visual stimulus was weak, compared to when it was strong. It is possible that these effects seen with the distracting stimulus may be similar to effects seen in task engagement. Where, the presence of the distracting visual stimulus actually causes somewhat less engagement with the auditory task by means of the distracting visual stimulus capturing some of the animals' attention. In future studies, it would be interesting to further delve into how distracting stimuli effect encoding in the auditory cortex; for instance, it would be interesting to see how the number of distracting stimuli effect encoding abilities.

In addition to the sensory aspect of these studies, we also investigated choice-related activity in auditory cortex. Our aims were to further disentangle choice-related activity from motor preparatory activity, as well as to elucidate whether this activity was due to feedforward sensory evidence, or various feedback mechanisms. Our findings suggest that choice-related activity is not simply reflective of motor-preparatory activity. In the feature-selective attention study, we found that neurons shifted their choice-related activity from increasing to decreasing for the same response motion between attention conditions. In both studies, we observed a greater population of neurons with choice-related activity during the response window (after stimulus offset, before response motion) than during the stimulus window. This is consistent with some previous studies of choice-related activity in auditory cortex (Bizley et al. 2013; Guo et al. 2019; Niwa et al. 2012b, 2013), although others have reported stronger choice-related activity during stimulus presentation (Christison-Lagay and Cohen 2018; Tsunada et al. 2016), though these tend to be later in the stimulus presentation of stimuli longer than those we presented in our studies. Our evidence seems to support that choice-related activity in auditory cortex is reflective of feedback from higher order areas where decision processes are occurring, whether those are higher-order auditory cortical areas or other areas such as prefrontal cortex. Further studies are necessary to further establish where these decision processes are occurring.

Finally, we sought to examine how attention and choice-related activity varied between two levels of the auditory hierarchy A1 and ML. We were surprised to find few differences between the two areas in both of our studies, as previous studies comparing A1 and ML found that task-engagement differentially effected AM detection encoding, the time-course of choice-related activity, and interneuronal correlated variability (Downer et al. 2017a; Niwa et al. 2013, 2015). It is possible that while we do not see differences between A1 and ML at the single neuron level, differences may be occurring related to attention and encoding at the population level. Future study of population level activity during similarly difficult selective attention tasks would be enlightening. Additionally, it is possible that sensory encoding is flexible dependent upon the demands of the task in terms of perceptual difficulty, stimulus ambiguity, and task difficulty. Which could make it necessary for the demands of sensory processing to be increased in higher order areas (such as ML) in order to effectively address the demands and thus may cause the encoding to look more similar between the two areas.

References

Atiani S, **David SV**, **Elgueda D**, **Locastro M**, **Radtke-Schuller S**, **Shamma SA**, **Fritz JB**. Emergent Selectivity for Task-Relevant Stimuli in Higher-Order Auditory Cortex. *Neuron* 82: 486–499, 2014.

Bagur S, **Averseng M**, **Elgueda D**, **David S**, **Fritz J**, **Yin P**, **Shamma S**, **Boubenec Y**, **Ostojic S**. Go/No-Go task engagement enhances population representation of target stimuli in primary auditory cortex. *Nat Commun* 9: 2529, 2018.

Bizley JK, **Walker KMM**, **Nodal FR**, **King AJ**, **Schnupp JWH**. Auditory Cortex Represents Both Pitch Judgments and the Corresponding Acoustic Cues. *Current Biology* 23: 620–625, 2013.

Buran BN, **von Trapp G**, **Sanes DH**. Behaviorally Gated Reduction of Spontaneous Discharge Can Improve Detection Thresholds in Auditory Cortex. *Journal of Neuroscience* 34: 4076–4081, 2014.

Carcea I, **Insanally MN**, **Froemke RC**. Dynamics of auditory cortical activity during behavioural engagement and auditory perception. *Nat Commun* 8: 14412, 2017.

Christison-Lagay KL, **Cohen YE**. The Contribution of Primary Auditory Cortex to Auditory Categorization in Behaving Monkeys. *Front Neurosci* 12: 601, 2018.

Downer JD, **Niwa M**, **Sutter ML**. Task Engagement Selectively Modulates Neural Correlations in Primary Auditory Cortex. *Journal of Neuroscience* 35: 7565–7574, 2015.

Downer JD, **Niwa M**, **Sutter ML**. Hierarchical differences in population coding within auditory cortex. *Journal of Neurophysiology* 118: 717–731, 2017a.

Downer JD, **Rapone B**, **Verhein J**, **O'Connor KN**, **Sutter ML**. Feature-Selective Attention Adaptively Shifts Noise Correlations in Primary Auditory Cortex. *The Journal of Neuroscience* 37: 5378–5392, 2017b.

Fritz J, **Shamma S**, **Elhilali M**, **Klein D**. Rapid task-related plasticity of spectrotemporal receptive fields in primary auditory cortex. *Nature Neuroscience* 6: 1216–1223, 2003.

Fritz JB, **Elhilali M**, **Shamma SA**. Adaptive Changes in Cortical Receptive Fields Induced by Attention to Complex Sounds. *Journal of Neurophysiology* 98: 2337–2346, 2007.

Guo L, **Weems JT**, **Walker WI**, **Levichev A**, **Jaramillo S**. Choice-Selective Neurons in the Auditory Cortex and in Its Striatal Target Encode Reward Expectation. *J Neurosci* 39: 3687–3697, 2019.

Lee C-C, **Middlebrooks JC**. Auditory cortex spatial sensitivity sharpens during task performance. *Nature Neuroscience* 14: 108–114, 2011.

Lin P-A, **Asinof SK**, **Edwards NJ**, **Isaacson JS**. Arousal regulates frequency tuning in primary auditory cortex. *Proc Natl Acad Sci USA* 116: 25304–25310, 2019.

Martinez-Trujillo JC, **Treue S**. Feature-Based Attention Increases the Selectivity of Population Responses in Primate Visual Cortex. *Current Biology* 14: 744–751, 2004.

Middlebrooks JC, **Dykes RW**, **Merzenich MM**. Binaural response-specific bands in primary auditory cortex (AI) of the cat: Topographical organization orthogonal to isofrequency contours. *Brain Research* 181: 31–48, 1980.

Miller JM, **Sutton D**, **Pfingst B**, **Ryan A**, **Beaton R**, **Gourevitch G**. Single Cell Activity in the Auditory Cortex of Rhesus Monkeys: Behavioral Dependency. *Science, New Series* 177: 449–451, 1972.

Ni AM, **Maunsell JHR**. Neuronal Effects of Spatial and Feature Attention Differ Due to Normalization. *J Neurosci* 39: 5493–5505, 2019.

Niwa M, **Johnson JS**, **O'Connor KN**, **Sutter ML**. Active Engagement Improves Primary Auditory Cortical Neurons' Ability to Discriminate Temporal Modulation. *Journal of Neuroscience* 32: 9323–9334, 2012a.

Niwa M, **Johnson JS**, **O'Connor KN**, **Sutter ML**. Activity Related to Perceptual Judgment and Action in Primary Auditory Cortex. *Journal of Neuroscience* 32: 3193–3210, 2012b.

Niwa M, **Johnson JS**, **O'Connor KN**, **Sutter ML**. Differences between Primary Auditory Cortex and Auditory Belt Related to Encoding and Choice for AM Sounds. *Journal of Neuroscience* 33: 8378–8395, 2013.

Niwa M, **O'Connor KN**, **Engall E**, **Johnson JS**, **Sutter ML**. Hierarchical effects of task engagement on amplitude modulation encoding in auditory cortex. *Journal of Neurophysiology* 113: 307–327, 2015.

Treue S, **Trujillo JCM**. Feature-based attention influences motion processing gain in macaque visual cortex. *Nature* 399: 575–579, 1999.

Tsunada J, **Liu ASK**, **Gold JI**, **Cohen YE**. Causal contribution of primate auditory cortex to auditory perceptual decision-making. *Nature Neuroscience* 19: 135–142, 2016.

Yin P, **Fritz JB**, **Shamma SA**. Rapid Spectrotemporal Plasticity in Primary Auditory Cortex during Behavior. *Journal of Neuroscience* 34: 4396–4408, 2014.